



Mobility & Vehicle Mechanics

*International Journal for Vehicle Mechanics, Engines and
Transportation Systems*

ISSN 1450 - 5304

UDC 621 + 629(05)=802.0

Saša Milojević Radivoje Pešić Dušan Gordić	NATURAL GAS AS A SAFE TECHNOLOGY FOR CLEAN URBAN VEHICLES	7-24
Saeed Abu Alyzeed Albatlan	INVESTIGATION OF PARAMETERS AFFECTING HYDRAULIC BRAKE LOAD SENSING VALVE PERFORMANCE	25-38
Gordana Bogdanović Dragan Milosavljević Ljiljana Veljović Aleksandar Radaković	COMPOSITE MATERIALS IN AUTOMOTIVE ENGINEERING MECHANICAL BEHAVIOR OF ANISOTROPIC MEDIA	39-49
Boris Rakić Lozica Ivanović Danica Josifović Blaža Stojanović	THE INFLUENCE OF VARIATION IN POSITION OF OUTPUT SHAFT TO LOAD ON THE CARDAN JOINT CROSS SHAFT	51-64



M V M

Mobility Vehicle Mechanics

Editors: Prof. dr Jovanka Lukić; Prof. dr Čedomir Duboka

MVM Editorial Board
University of Kragujevac
Faculty of Engineering
Sestre Janjić 6, 34000 Kragujevac, Serbia
Tel.: +381/34/335990; Fax: + 381/34/333192

Prof. Dr **Belingardi Giovanni**
Politecnico di Torino,
Torino, ITALY

Dr Ing. **Ćučuz Stojan**
Visteon corporation,
Novi Jicin,
CZECH REPUBLIC

Prof. Dr **Demić Miroslav**
University of Kragujevac
Faculty of Engineering
Kragujevac, SERBIA

Prof. Dr **Fiala Ernest**
Wien, OESTERREICH

Prof. Dr **Gillespie D. Thomas**
University of Michigan,
Ann Arbor, Michigan, USA

Prof. Dr **Grujović Aleksandar**
University of Kragujevac
Faculty of Engineering
Kragujevac, SERBIA

Prof. Dr **Knapezyk Josef**
Politechniki Krakowskiej,
Krakow, POLAND

Prof. Dr **Krstić Božidar**
University of Kragujevac
Faculty of Engineering
Kragujevac, SERBIA

Prof. Dr **Mariotti G. Virzi**
Universita degli Studidi Palermo,
Dipartimento di Meccanica ed
Aeronautica,
Palermo, ITALY

Prof. Dr **Pešić Radivoje**
University of Kragujevac
Faculty of Engineering
Kragujevac, SERBIA

Prof. Dr **Petrović Stojan**
Faculty of Mech. Eng. Belgrade,
SERBIA

Prof. Dr **Radonjić Dragoljub**
University of Kragujevac
Faculty of Engineering
Kragujevac, SERBIA

Prof. Dr **Radonjić Rajko**
University of Kragujevac
Faculty of Engineering
Kragujevac, SERBIA

Prof. Dr **Spentzas Constantinos**
N. National Technical University,
GREECE

Prof. Dr **Todorović Jovan**
Faculty of Mech. Eng. Belgrade,
SERBIA

Prof. Dr **Toliskyj Vladimir E.**
Academician NAMI,
Moscow, RUSSIA

Prof. Dr **Teodorović Dušan**
Faculty of Traffic and Transport
Engineering,
Belgrade, SERBIA

Prof. Dr **Veinović Stevan**
University of Kragujevac
Faculty of Engineering
Kragujevac, SERBIA

For Publisher: Prof. dr Miroslav Babić, dean, University of Kragujevac, Faculty of Engineering

***Publishing of this Journal is financially supported from:
Ministry of Education, Science and Technological Development, Republic Serbia***

MVM – International Journal for Vehicle Mechanics, Engines and Transportation Systems
NOTIFICATION TO AUTHORS

The Journal MVM publishes original papers which have not been previously published in other journals. This is responsibility of the author. The authors agree that the copyright for their article is transferred to the publisher when the article is accepted for publication.

The language of the Journal is English.

Journal *Mobility & Vehicles Mechanics* is at the SSCI list.

All submitted manuscripts will be reviewed. Entire correspondence will be performed with the first-named author.

Authors will be notified of acceptance of their manuscripts, if their manuscripts are adopted.

INSTRUCTIONS TO AUTHORS AS REGARDS THE TECHNICAL ARRANGEMENTS OF MANUSCRIPTS:

Abstract is a separate Word document, “*First author family name_ABSTRACT.doc*”. Native authors should write the abstract in both languages (Serbian and English). The abstracts of foreign authors will be translated in Serbian.

This document should include the following: 1) author’s name, affiliation and title, the first named author’s address and e-mail – for correspondence, 2) working title of the paper, 3) abstract containing no more than 100 words, 4) abstract containing no more than 5 key words.

The manuscript is the separate file, „*First author family name_Paper.doc*“ which includes appendices and figures involved within the text. At the end of the paper, a reference list and eventual acknowledgements should be given. References to published literature should be quoted in the text brackets and grouped together at the end of the paper in numerical order.

Paper size: Max 16 pages of B5 format, excluding abstract

Text processor: Microsoft Word

Margins: left/right: mirror margin, inside: 2.5 cm, outside: 2 cm, top: 2.5 cm, bottom: 2 cm

Font: Times New Roman, 10 pt

Paper title: Uppercase, bold, 11 pt

Chapter title: Uppercase, bold, 10 pt

Subchapter title: Lowercase, bold, 10 pt

Table and chart width: max 125 mm

Figure and table title: Figure _ (Table _): Times New Roman, italic 10 pt

Manuscript submission: application should be sent to the following e-mail:

mvm@kg.ac.rs ; lukicj@kg.ac.rs

or posted to address of the Journal:

University of Kragujevac – Faculty of Engineering

International Journal M V M

Sestre Janjić 6, 34000 Kragujevac, Serbia

The Journal editorial board will send to the first-named author a copy of the Journal offprint.

OBAVEŠTENJE AUTORIMA

Časopis MVM objavljuje originalne radove koji nisu prethodno objavljivani u drugim časopisima, što je odgovornost autora. Za rad koji je prihvaćen za štampu, prava umnožavanja pripadaju izdavaču.

Časopis se izdaje na engleskom jeziku.

Časopis *Mobility & Vehicles Mechanics* se nalazi na SSCI listi.

Svi prispeli radovi se recenziraju. Sva komunikacija se obavlja sa prvim autorom.

UPUTSTVO AUTORIMA ZA TEHNIČKU PRIPREMU RADOVA

Rezime je poseban Word dokument, „*First author family name_ABSTRACT.doc*“. Za domaće autore je dvojezičan (srpski i engleski). Inostranim autorima rezime se prevodi na srpski jezik. Ovaj dokument treba da sadrži: 1) ime autora, zanimanje i zvanje, adresu prvog autora preko koje se obavlja sva potrebna korespondencija; 2) naslov rada; 3) kratak sažetak, do 100 reči, 4) do 5 ključnih reči.

Rad je poseban fajl, „*First author family name_Paper.doc*“ koji sadrži priloge i slike uključene u tekst. Na kraju rada nalazi se spisak literature i eventualno zahvalnost. Numeraciju korišćenih referenci treba navesti u srednjim zagradama i grupisati ih na kraju rada po rastućem redosledu.

Dužina rada: Najviše 16 stranica B5 formata, ne uključujući rezime

Tekst procesor: Microsoft Word

Margine: levo/desno: mirror margine; unurašnja: 2.5 cm; spoljna: 2 cm, gore: 2.5 cm, dole: 2 cm

Font: Times New Roman, 10 pt

Naslov rada: Velika slova, bold, 11 pt

Naslov poglavlja: Velika slova, bold, 10 pt

Naslov potpoglavlja: Mala slova, bold, 10 pt

Širina tabela, dijagrama: max 125 mm

Nazivi slika, tabela: Figure __ (Table __): Times New Roman, italic 10 pt

Dostavljanje rada elektronski na E-mail: mvm@kg.ac.rs ; lukicj@kg.ac.rs

ili poštom na adresu Časopisa
Redakcija časopisa M V M
Fakultet inženjerskih nauka
Sestre Janjić 6, 34000 Kragujevac, Srbija

Po objavljivanju rada, Redakcija časopisa šalje prvom autoru jedan primerak časopisa.

Mobility &

Motorna

Vehicle

**Volume 39
Number 1
2013.**

Vozila i

Mechanics

Motori

Saša Milojević Radivoje Pešić Dušan Gordić	NATURAL GAS AS A SAFE TECHNOLOGY FOR CLEAN URBAN VEHICLES	7-24
Saeed Abu Alyazeed Albatlan	INVESTIGATION OF PARAMETERS AFFECTING HYDRAULIC BRAKE LOAD SENSING VALVE PERFORMANCE	25-38
Gordana Bogdanović Dragan Milosavljević Ljiljana Veljović Aleksandar Radaković Mirjana Lazić	COMPOSITE MATERIALS IN AUTOMOTIVE ENGINEERING – MECHANICAL BEHAVIOR OF ANISOTROPIC MEDIA	39-49
Boris Rakić Lozica Ivanović Danica Josifović Blaža Stojanović Andreja Ilić	THE INFLUENCE OF VARIATION IN POSITION OF OUTPUT SHAFT TO LOAD ON THE CARDAN JOINT CROSS SHAFT	51-64

Mobility &

Vehicle

Mechanics

Motorna

Vozila i

Motori

**Volume 39
Number 1
2013.**

Saša Milojević Radivoje Pešić Dušan Gordić	PRIRODNI GAS KAO BEZBEDNA TEHNOLOGIJA ZA ČISTIJA GRADSKA VOZILA	7-24
Saeed Abu Alyazeed Albatlan	ISTRAŽIVANJE PARAMETARA KOJI UTIČU NA PERFORMANSE KOČNOG VENTILA OSETLJIVOG NA OPTEREĆENJE	25-38
Gordana Bogdanović Dragan Milosavljević Ljiljana Veljović Aleksandar Radaković Mirjana Lazić	KOMPOZITNI MATERIJALI U AUTOMOBILSKOJ INDUSTRIJI - MEHANIČKO PONAŠANJE ANIZOTROPNE SREDINE	39-49
Boris Rakić Lozica Ivanović Danica Josifović Blaža Stojanović Andreja Ilić	UTICAJ PROMENE POLOŽAJA GONJENOG VRATILA NA OPTEREĆENJE KRSTASTE OSOVINE KARDANSKOG PRENOSNIKA	51-64

¹NATURAL GAS AS A SAFE TECHNOLOGY FOR CLEAN URBAN VEHICLES

Saša Milojević, Radivoje Pešić, Dušan Gordić

UDC: 629.1.07

Summary

A motor vehicle fuel can be dangerous if handled improperly. Like liquefied petroleum gas, gasoline and diesel fuel are potentially dangerous fuels, but over time we are learned to use them safely. The same is true with natural gas. It safely generates our electricity, heats our homes and cooks our meals. Natural gas from the gas field to the vehicle's engine, requires very little processing to make it suitable for the use as a fuel. Usually, at a reciprocating compressor's fueling station, the natural gas is compressed and provided to vehicles, where it is stored at 200 bar pressure like Compressed Natural Gas (CNG). In the paper, the solutions for the safe conversion of gasoline powered car and local articulated bus to dedicated Natural Gas Vehicle (NGV) are shown. In addition to safety, the paper demonstrates also ecological benefits, regarding to the use of NGVs in urban transport. In the paper, shortly is presented a look in the natural gas market and safety regulations.

Key words: Compressed natural gas, safe vehicle, cleaner urban transport.

PRIRODNI GAS KAO BEZBEDNA TEHNOLOGIJA ZA ČISTIJA GRADSKA VOZILA

UDC: 629.01;681.5.015.87

Rezime

Svako gorivo može biti opasno ako se koristi nepravilno u motornom vozilu. Tečni naftni gas, benzin i dizel su takođe potencijalno opasna goriva, ali smo vremenom naučili da ih bezbedno koristimo. Isto važi i za prirodni gas. On se bezbedno koristi za proizvodnju struje, za grejanje stanova i pripremu hrane. Prirodni gas sa nalazišta zahteva mali tretman da bi mogao da se koristi kao gorivo za motore. Obično se prirodni gas komprimuje uz pomoć klipnih kompresora do pritiska od 200 bar i kao komprimovan (CNG) se skladišti u vozilima. U radu su prikazane solucije za konverziju automobila i gradskog zglobnog autobusa na prirodni gas. Dodatno, pored bezbednosti prikazane su i ekološke prednosti vozila na prirodni gas u saobraćaju. Ukratko je prikazana dinamika na tržištu prirodnog gasa i sistematizovani su propisi koji se odnose na bezbednost

Ključne reči: Komprimovani prirodni gas, bezbedno vozilo, čistiji gradski saobraćaj

¹ *Received November 2012, Accepted: January 2013.*

NATURAL GAS AS A SAFE TECHNOLOGY FOR CLEAN URBAN VEHICLES

Saša Milojević¹, M.Sc. PhD Student, Radivoje Pešić, Full Professor, Dušan Gordić, Full Professor

UDC: 629.1.07

1. INTRODUCTION

Natural gas is a fossil fuel of choice for Europe. It is clean, safe, and available fuel with a acceptable price for the region's residential, industrial, and commercial customers [2,5,8].

Today the natural gas consumption shows an increase after the global economic crisis. World natural gas consumption grew by 7.4% in 2010, with above-average growth in all regions. The US had the world's largest 2010 increase in consumption, rising by 5.6% to a new record high. Russia and China also registered large increases – the largest volumetric increases in the country's history in each case. Consumption in other Asian countries also grew rapidly in 2010 (+10.7%), led by a 21.5% increase in India. EU27 countries also show an increase of 7.2% in 2010 in total natural gas consumption, compared to 2009 [11,14].

Natural gas production in North Sea and other EU countries will continue providing significant amounts of gas for Europe's needs. According to the latest estimates by the International Energy Agency, natural gas consumptions in the EU will be increased from 536 billion cubic meters (bcm) in 2008 to 636 bcm in 2035 – an increase of 19%. By 2035, EU domestic gas production will have dropped up to about 50%. In that situations, the Russian Federation has the choice to fill a significant proportion of the EU import gap of 113 to 155 bcm by the year 2030 [11].

The South Stream Offshore Gas Pipeline is important in terms of efficiency and stable supply of the gas market. The project will contribute to EU energy security, like in the Republic of Serbia too, and will help to meet their Carbon Dioxide (CO₂) reduction targets.

The projected 63 bcm of natural gas per year transported via pipeline is equivalent to [11]:

- The same energy as 50.000 wind turbines,
- The energy of 38 nuclear power plants,
- Provides the energy needed for about 30 million European households,
- Accounts for approximately 10% of the total EU gas consumption,
- Delivers the same amount of energy as 420 Liquefied Natural Gas tankers, and
- Delivers the same amount of energy like approximately 550 oil tankers that could be challenging crude oil transportation exercise given the intense maritime traffic in the Black Sea and in the Bosphorus Strait.

The transport sector, which relies heavily on cars and trucks, is responsible for about a quarter of the world's energy use and has the fastest rising of carbon emission

¹ Saša Milojević, M.Sc., University of Kragujevac, Faculty of Engineering, tiv@kg.ac.rs

regarding to any economic sector. Road transport currently accounts for 74% of the world's total transport-related (CO₂) emissions [8,13].

The world's fleet of vehicles is passed number of one billion (1.015 billion in 2010, 752 million in 2000 and a mere 127 million in 1960), while the production capacities of the world's auto companies was estimated to grow to 97 million units per year by 2015 (the estimations are before the global economic crisis in 2009) [13].

Natural gas as fuel for motor vehicles has more and more share. The consequences to this fact are that today world has approx. 15.1 million of NGVs (half million of the CNG buses and 14.1 million of cars and light duty vehicles), and over 20.500 filling stations [1].

According to this trend, the policy developments will also influence on the future gas demands, including the EU's adoption to the future emission targets. These cannot be achieved without using of natural gas as a substitute for fuels that creating more pollution in the vehicles. Natural gas is essential for maximizing the reduction of carbon and rest exhaust emissions rapidly at a relatively small cost of the substitution process.

Regarding to the rise of natural gas application like engine fuel and importance of the topic, in the paper is preferred to find a replay on the question: (How Safe is NGV?). The analyses in the paper are confirmed on the examples of the vehicles converted for CNG drive.

2. NATURAL GAS AS FUEL FOR MOTOR VEHICLES

All gases are good fuels for Otto engines: a mixture with air is high quality and ready for complete combustion, the work of engine is economical, with lower exhaust emissions and extended oil and engine life.

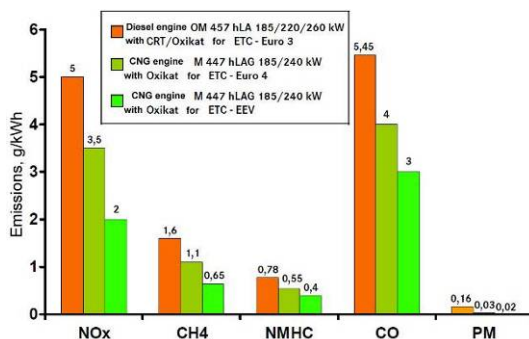
Natural gas is a naturally occurring fuel which requires little processing before use. Chemically it consists of 90% methane with smaller amounts of ethane, propane, butane, CO₂, and other trace gases. The high methane content gives natural gas its high octane rating (120-130) and clean-burning characteristics, allowing high engine efficiency and low emissions. The environmental benefit of using CNG, as fuel is the reduction of exhaust gases in articulated bus for example, Figure 1. Compared to the equivalent Turbo Diesel Engine, carbon monoxide (CO) emissions are over 50% lower, nitrogen oxide (NO_x) emissions are 80% lower, and there are around zero particulates [4].

Lean-burn heavy-duty CNG engines were initially popular due to their lower engine-out NO_x emissions and higher fuel efficiency compared to stoichiometric engines. A modern, closed-loop electronically controlled lean-burn CNG engine can achieve Euro V or lower emission levels for both NO_x and PM. For optimal emission performances, these engines should be also equipped with natural gas-optimized oxidation catalyst after-treatment.

To meet the most stringent Euro VI emission standard for NO_x, it is necessary to switch to stoichiometric combustion combined with exhaust gas recirculation and three-way catalyst after-treatment.

From the other side, it is notable that natural gas in normal conditions has a low density of energy per unit volume. To meet all requirements needed to become engine fuel, it shall be a subject to appropriate treatment. The easiest way is to use CNG stored under high pressure into cylinders on the vehicle (working pressure of 200 bar). Another possibility for increasing the energy density of natural gas in the fuel tank is its conversion

into liquid form through the cooling up to -162 °C, and storing it into cryogenic cylinders like Liquefied Natural Gas (LNG).



*CRT[®] - (Continuously Regenerating Technology) particulate filter
ETC-European Transient Cycle, EEV- Enhanced environmentally friendly vehicle*

Figure 1: Exhaust emissions reduction of 12 liters engine in EvoBus

Before discussing the NGV design, it is very important to understand some relevant properties of natural gas like vehicle fuel what makes this fuel different from gasoline or diesel. The items below summarize the basic differences between the properties of gaseous and liquid fuels that influence the NGV design changes:

- It is non-toxic, neither carcinogenic nor corrosive gas, but it is the stuffy,
- Natural gas is invisible but must be odorized so its presence can be detected,
- Unlike gasoline vapors, natural gas is lighter than air (methane has density of 0.68 kg/m³ at 15 °C) and it is in the gaseous form at atmospheric conditions. In an event of a leak, this property allows to quickly rise in the atmosphere, while the propane (1,87 kg/m³) and butane (2,44 kg/m³) are heavy than air, and lower to floor,
- Natural gas has an auto ignition temperature of around 480 to 650 °C whereas gasoline is approximately 260 to 430 °C and diesel less than 260 °C. This relatively high auto ignition temperature for CNG is an additional safety feature of this fuel, and
- Methane has a very selective range of flammability. The mixture of gas in air by volume that will support combustion is between 4.4 and 15%. In other words, with less than 4.4%, of the methane in air, the mixture will not burn because it is too lean, and with greater than 15%, the mixture is too rich and will not burn. Ignitable range for gasoline is between 1.4 and 7.6% and around 0.6 to 7.5% for diesel.

Modification of the vehicle and engine to natural gas drive can affect:

- Emissions/air quality, and
- Performance, durability, and safety of engine /turbine/ generator / and other systems.

Quality can be described in two ways:

- Composition – chemical breakdown of components, and
- Performance – how the gas behaves in various circumstances. Some common measures of gas performance include heating value (Btu), Wobbe number, and methane number (MN). Gas performance can be managed by alteration of its content.

There are three national and only one international standard for natural gas vehicle fuel:

- SAE J1616: Recommended Practice for Compressed Natural Gas Vehicle Fuel,
- DIN 51624: Automotive Fuels - Compressed Natural Gas - Requirements And Test Methods,
- 13 CCR § 2292.5 (California Code of Regulations) Specifications for Compressed Natural Gas, and
- ISO/TR 15403-2:2006 addresses the specifications of natural gas as a compressed fuel for vehicles as an addendum to ISO 15403-1. Specifically, ISO/TR 15403-2:2006 is intended to satisfy requests for quantitative data.

3. EXISTING TECHNICAL SOLUTIONS FOR NGV

Substitution of existing fuels by natural gas in road transport can be realized by introducing of new vehicles equipped with original CNG engines, or as a first step, by converting engines of existing vehicles to CNG drive. To introduce natural gas as a fuel for road transport, the following options are possible:

- Modification of a gasoline engine to CNG combustion (so called conversion to a dedicated fuel),
- Modification of a gasoline engine to either CNG or gasoline (two way/bi-fuel) combustion,
- Conversion of a diesel engine to dedicated CNG (spark ignition) combustion, and
- Conversion of a diesel engine to dual fuel (gas and diesel combined) combustion.

Figure 2 shows typical components associated with a CNG vehicle fuel system for sequential injection. These are basic elements and some system manufacturers may add other components.

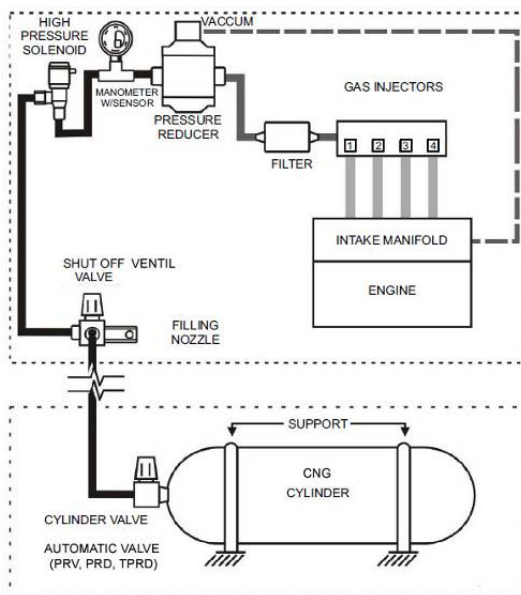


Figure 2: Typical CNG Vehicle Fuel System

3. 1 EXAMPLE OF PASSENGER CAR WITH CNG DRIVE

Conversion of gasoline vehicles has been successfully carried out for decades in many countries worldwide, mostly stimulated due to a price advantage of CNG over gasoline.

Strength construction in combination with the optimum use of interior space is a basic demand for NGV. Like example on the Figure 3 is presented a concept of the vehicle type Zafira 1.6 CNG [7], where are mounted CNG cylinders (two in front and two behind of the rear axle). For the reserve drive, between is mounted a gasoline tank.

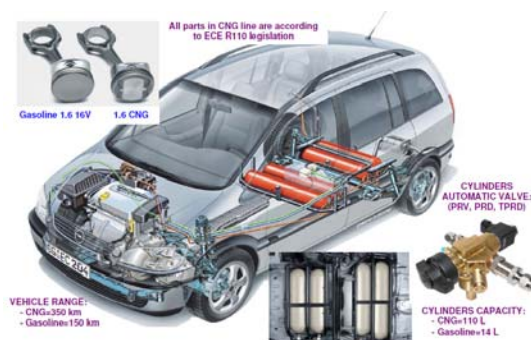


Figure 3: Bi-fuel vehicle

The mounted CNG cylinders are made of special steel, designed for working gas pressure of 200 bar. Prior to installation, each cylinder is separately checked under a pressure of 300 bar [7]. For additional protection in the event of an accident, the cylinders are mounted in safety cover made of steel used for racing vehicles.

Each of the cylinders is fitted with an automatic valve with the following safety features:

- The electrically controlled solenoid valve releases the flow of gas only when the ignition is switched on. In the case of an accident, or if the engine stops, all four solenoid valves will be closed,
- An integrated check valve automatically switches-off the flow of gas in the event of the pressure drop in the gas cylinders, caused by a leaking connection,
- In the event of a vehicle fire, an integrated melt fuse ensures a controlled release of natural gas if the temperature exceeds 110 °C,
- If pressure rises over a defined limit, an additional burst valve also ensures controlled release of gas, and
- Each gas flow from the cylinder is possible to stop by using a manual cut-off valve.

Because natural gas has an octane, value of up to 130, it is significantly less liable to cause engine knocking than gasoline. This means that the efficiency of vehicle is rising correspondingly by increasing the compression ratio. The Zafira 1.6 CNG has special pistons designed for natural gas operation. With the raised areas on the piston, heads increased the compression ratio to (12.5:1). This makes it possible to exploit the higher-octane content of natural gas, and consequently to boost operating efficiency. In addition to

the pistons, the valves, valve guides and valve sets of the Zafira 1.6 CNG were configuring specifically for natural gas operation [7].

The Zafira 1.6 CNG has unlike other natural gas vehicles a dual injection bank with four injection nozzles for natural gas and gasoline.

As a result, in conjunction with a special injection system and engine management in dedicated fuel operations, achieved nearly the same performances as in the case of the drive with the gasoline engine type 1.6 16V ECOTEC®.

According to the information received in the vehicle's exploitations, four capacious CNG cylinders ensure a drive range of approximately 350 km in natural gas operation. An additional reserve gasoline tank with the capacity of 14 liters mounted between the gas cylinders below the floor [7]. If need be, however, the reserve gasoline tank ensures an additional range of approximately 150 km, enough to bridge all gaps in the CNG supply network.

3. 2 PROJECT PROPOSITION FOR THE CONVERSION OF ARTICULATED BUS TO CNG DRIVE

For buses, driven by diesel engine, there are two options for conversion on CNG drive: conversion for dedicated or dual fuel combustion. The option can be selected, depending on the engine characteristics and the working conditions (routes, working time, available refueling network etc.).

City buses circulate from a garage to the destination places on unchangeable routes. Those are favorable conditions regarding to the needs of the transport logistics, specifically regarding to the paining of the refueling time and place. That is very important for territories with the limited gas network.

According to the mentioned and any other facts, the city buses are suitable for drive with engines on dedicated CNG combustion. Like first example, in existing diesel buses, the diesel engine must be modified to a spark ignition engine in order to burn natural gas instead of diesel. The major modification is a reduction of the compression ratio to approximately 14:1, while the cooling system of the engine has to be improved. Diesel injectors must be replaced with spark plugs and according to this; the high-pressure pump for diesel fuel needs to be replaced with the spark ignition coil(s), too. Additionally, a voltage converter from the standard 24 V system used on vehicles equipped with diesel engines to a 12 V system is required. For this reconstruction can be used a set of parts and instructions for the diesel engine reconstruction of the company Omnitek Engineering Corp. (OEC).

Secondly, from our side the best variant is the using of the completely new engine with dedicated CNG combustion, which is paired with automatic gearbox and driven axle. It is accepted the propositions for the bus drive unit with original engine and gearbox. The natural gas engine type is M 447 hLAG spark ignited, Figure 4. That engine is designed to meet the EEV emission standards, by applications of a single point injection of fuel, in combinations with lean burn combustion and oxidation catalyts. The engine is based on the 12 liters diesel automotive OM 457-hLA platform and shares many installation options with the diesel counterpart. In combination with the automatic gearbox DC, achieved good performance of movement and maximum use of engine output parameters, which have a positive effect on passengers comfort and fuel economy.

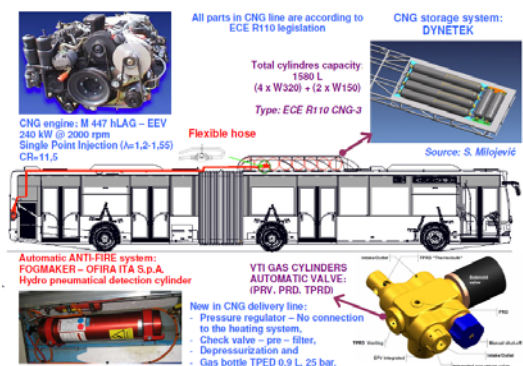


Figure 4: The design of CNG line applied on the articulated bus

In the bus, body can be integrated modern automatic anti fire system mark Fogmaker – Ofira, with hydro pneumatically activated detection cylinder.

The retrofit of the diesel bus into a dedicated NGV begins with the joining of the CNG cylinders with the original rack to the bus roof, Figure 4. For prototype vehicle, we are mounted four cylinders DYNETEK type "W320" and two of type "W150", with a total water capacity of 1.580 L. The selected CNG storage system includes type 3 cylinders composed of an aluminum liner (brand Dyncell®), with a favorable ratio between weight and volume (0.3 kg/L to 0.4 kg/L), [5,6,10]. During the conversion, we have considered the existing regulations regarding the dimensions and gross vehicle weight. Specifically, we took into account the requirements relating to the correct joining of the main parts of the CNG fuel line and gas cylinders, all legislated by regulation ECE R 110 [6,12].

4. GAS MARKET SUPPLY AND CNG VEHICLES FILLING

The South Stream project has a goal to ensure the EU energy security. This project is required to continue the introductions of NGVs in our country too [11].

To secure natural gas supply, like the bridge before gas networking (applicable for any territories), is better to use the Containers for CNG Bulk transport with trailers Figure 5. Analyzed Containers for Gas Transport are approved by TÜV according to ADR as MEGC, with the next main characteristics, Table 1 [3,9,10]:

- Extremely High Storage Capacity due to Light-Weight Composite Cylinders,
- Low Weight, Less Wear and Friction = Lower Costs for Maintenance and Repair,
- Handling by Crane/Forklift, and attaching to the trailer by ISO corner castings,
- Lifetime up to 40 years,
- Standard 250 bar Service Pressure,
- Vertical or Horizontal Assembly with Neck or Belly Mounting,
- Leak test at service pressure N₂, helium leak test at 2 bar,
- Higher filling level during rapid filing at high gas temperature (Al 6061 liner high heat-conductivity), and
- Cylinders type-3 (Al 6061 liner) is Corrosion Free with respect to Steel cylinder or Jumbo Vessel Trailer.



(a) ISO 20 ft Container



(b) 10 ft Cube for Bulk Transport

Figure 5: The 250 bar Modules**Table 1: ISO 20 ft and 40 ft Container Options DYNETEK**

TYPE OF CYLINDERS	Composite Type-3 20 ft Container 1CC 250 bar	Composite Type-3 40 ft Container 1CC 250 bar	Jumbo Vessels 40 ft Semi trailer 250 bar
<u>A. Cylinder Material</u>	Al 6061 liner + Carbon Fiber in Epoxy Resin		Steel 34CrMo4
Standard	TPED / ADR		
No. of Cylinders	76	152	9
Outside diameter	406 mm		559 mm
Cylinder capacity	234 L		2385 L
Cylinder Weight	82 kg		2660 kg
Test pressure	375 bar		300 bar
Total Cylinder Volume	17784 L	35568 L	21400 L
<u>B. Weights</u>			
Total Cylinder weight	6232 kg	12464 kg	23940 kg
Total gas weight *	4222 kg	8444 kg	4471 kg
Total Trailer Weight Full Container	Approx. 14.5 t	Approx. 29.4 t	Max. 40 t

*depending on actual density of CNG used and filling conditions!

TPED - Transportable Pressure Equipment Directive,

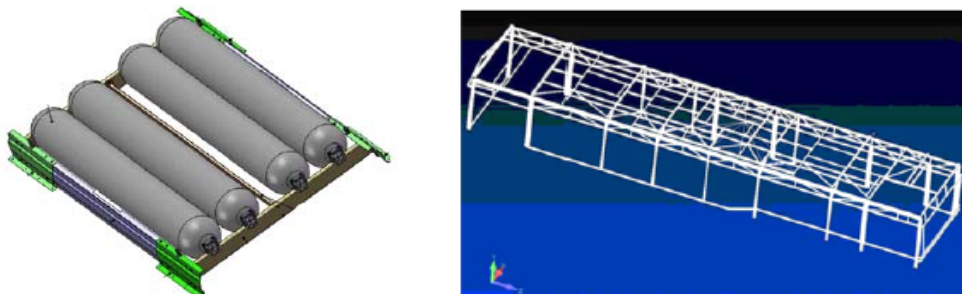
ADR - European Agreement concerning the International Carriage of Dangerous Goods by Road, and

MEGC - Multi Elements Gas Container.

5. INSPECTION OF THE NATURAL GAS VEHICLES AND CYLINDERS

The principal requirement for NGV of the M3 and N3 categories is the strength at destruction of the joint assembly between the CNG cylinders and the chassis during a deceleration of 6.6-g in the longitudinal direction and 5-g in the transverse direction (UN ECE No. 110, 2008; ISO/DIS 11439, 2000). The standard ECE R 110 legislates the proofing of these requirements using calculations rather than experimental testing [12].

Like example, on the Figure 6 are presented standard CNG cylinders rack and a generic model of bus, which includes the supporting structures to a level below the windows [6].



(a) CNG cylinders rack DYNETEK V294

(b) Model of the supporting bus structure

Figure 6: The standard CNG cylinders rack and a generic model of bus

6. REGULATIONS RELATING ON THE INSPECTION OF NGV

6.1 INTERNATIONAL REGULATIONS

Regulation and standards for natural gas vehicles are shown on Figure 7.

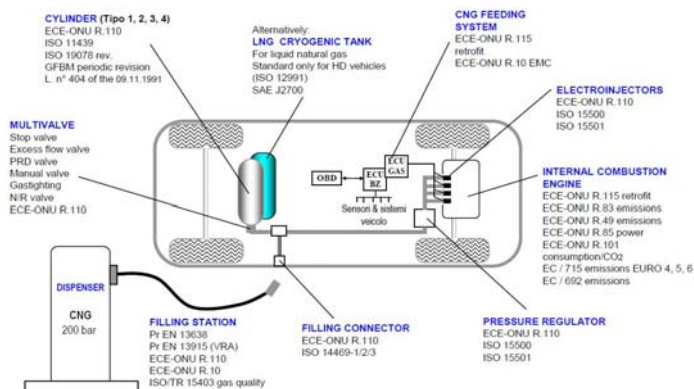


Figure 7: Regulations and standards for natural gas vehicles

Ecological demands relating on CNG truck and buses are defined in ECE Regulation No. 49. For passenger cars, those demands are defined in ECE Regulation No. 83.

Safety and demands regarding to mounting propriety of CNG equipments, also relating on gas driven vehicles are defined in the next two Regulations [12]:

1. UN ECE Regulation No. 110 – uniform homologation provisions concerning the approval of:
 - Specific components of motor vehicles using CNG in their propulsion system, and

- Vehicles with regard to installation of specific components of an approved type for the use of CNG in their propulsion system.
2. UN ECE Regulation No. 115 – uniform homologation provisions concerning the approval of:
- Specific LPG (liquefied petroleum gases) retrofit systems to be installed in motor vehicles for the use of LPG in their propulsion system, and
 - Specific CNG (compressed natural gas) retrofit systems to be installed in motor vehicles for the use of CNG in their propulsion system.

6.2 NATIONAL REGULATIONS

In the Republic of Serbia for gas driven vehicles are applicable the next Regulation and under Regulation acts:

- Law about traffic safety on the roads (Republic of Serbia, Official carrier No. 41/09 and 53/10),
- Rulebook about partition of motor vehicles and trailers and technical demands for the vehicles in the traffic on roads (Republic of Serbia, Official carrier No. 64/10. and 69/10), and
- Rulebook about vehicles testing (Republic of Serbia, Official carrier No. 8/12).

7. INSPECTION AND MAINTENANCE OF CYLINDERS AND CONNECTING ELEMENTS

7.1 CYLINDER DESCRIPTION

DyneCell® cylinders, which here analyzed are type-3 fully wrapped. Those cylinders consist of a seamless 6061 aluminum liner, which is fully wrapped with a carbon fiber, and epoxy reinforced laminate, Figure 8 (a) [10]. Figure 8 (b) illustrates the cross section of cylinder with reinforced neck, checked in vibrations. Comparing with type-4 cylinders of plastic liner, those type-3 cylinders after strong and vibration tests have not the problems like as the leakage because of cracks under thermal and mechanical stresses [10].

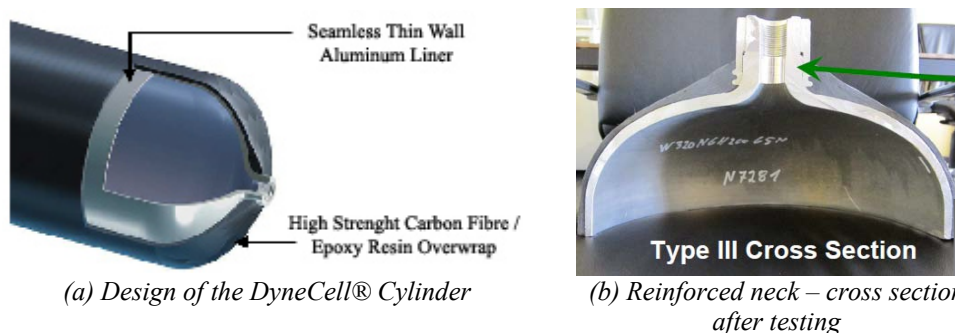


Figure 8: DyneCell® cylinder cross section before and after testing

DyneCell® cylinders are designed to work under the nominal service pressure of 20 MPa (200 bar) at an ambient temperature of 15 °C. In the real situations, at filling, the pressure to be dispensed shall be calculated giving consideration to gas temperature in order to prevent pressures exceeding the maximum allowable filling condition. The following approximation calculations, represented with equation 1 may be helpful here [3,10]:

$$\text{Pressure of CNG bar} = 176 + 1.6 \times (\text{Temperature of CNG } ^\circ\text{C}) \quad (1)$$

The actual pressure of CNG in cylinder also depends, however, on the relevant gas composition.

The maximum filling pressure may not exceed 26 MPa (260 bar) at any temperature. Cylinders shall not be connected to compressors at filling stations with maximum output pressures greater 1.5 times of nominal value.

Settled temperature of gases in cylinders may vary from a low of -40 °C to a high of 65 °C. The temperature of the cylinder materials may vary from -40 °C to 82 °C. Temperatures over 65 °C shall be sufficiently y local, or of short enough duration, that the temperature of gas in the cylinder never exceeds 65 °C [3,10].

CNG shall comply with gas compositions specified in ISO 11439 respective UN ECE Regulation No. 110 [12].

The cylinders have a maximum Service Life of 15 to 20 years from the final manufacturing inspection date, depending on the number of cycles per year specified in the relevant standard for the country where the cylinder is operated. The expiration date is specified on the label.

When the Service Life is reached, the cylinders must be removed from service. If cylinders are filled more than (1000 x Service Life in years) before the expiration date is reached the cylinders must be removed from service [3,10].

7. 2 INSTALLATION REQUIREMENTS

The Neck Mount Brackets securely fasten the DyneCell® cylinders Figure 9 for cylinder rack like on Figure 6 (a) on board automotive vehicles Figure 4 in a horizontal position. Cylinders are mounted using the two different neck-mounting brackets that secure the extended necks. One end of the cylinder is held secure while the other end is allowed to slide as the cylinder expands, adjusting for temperature and pressure variations.

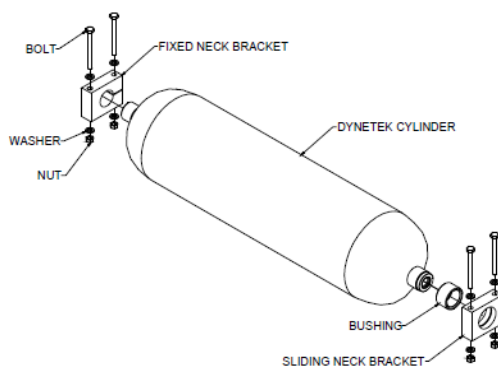


Figure 9: Cylinders with Neck Mount Assembly

When the brackets are installed, the fixed neck mount bracket locks the cylinders neck against sliding in the bracket up to a longitudinal load of 17 kN. This is equal to the following weights of a filled cylinder, Table 2 [3,10,]:

Table 2: Allowed total weight of cylinders according to UN ECE R110

Vehicle category	M1 or N1	M2 or N2	M3 or N3
Acceleration	20·g	10·g	6,6·g
Max. allowed total cylinder weight *	86 kg	173 kg	262 kg

* Max. total cylinder weight = 17 kN / (9,81 m/s² x acceleration)

7. 3 INSPECTION AND RETESTING REQUIREMENTS

Cylinders require an external visual re-inspection for defects in the composite wrap at certain intervals after installation or upon reinstallation. Inspection shall always be in accordance with the relevant standards and regulations of the country where the cylinder is operated.

According to UN ECE R110, for natural gas cylinders this inspection shall be performed at least every 48 months after the date the vehicle enters into service [12]. Other cylinders may have shorter inspection intervals depending on the relevant standard. Also any requirements due to the type approval need to be respected.

Inspection shall be in accordance with procedures outlined in ISO 19078, and/or also according to the relevant national standard of the country where the cylinder is operated [3]. If a hydraulic pressure test is to be performed for retesting, this may only be done using specially treated water (use of inhibitors, removal of chloride etc.). Also, recommended to use shortest possible time of exposure and never fill the cylinders with ordinary water since there is a risk of damaging the aluminum liner material due to tap Water corrosion.

An inspection is an important safety measure to detect whether the cylinder or mounting system is damaged, and to ensure that it is not suffering from a harmful environment during operation. Inspections should be conducted with the proper tools, which may include measuring tools to measure flaw length and depth, a flashlight etc. There are two types of inspections, General Inspection and Certification Inspection as summarized by Table 3, [3].

Table 3: Summary of Inspection Categories

Inspection Type	Inspection Description	Inspection Frequency
General Inspection	Performed by the driver, maintenance personnel, or other service technician. It is primarily a visual inspection to ensure that the cylinder, mounting and piping are in good condition and secure.	Recommended every 3 months
Certification Inspection	Performed by trained personnel who are certified in accordance with the local regulations and authorities. It is a more detailed examination of the cylinder, mounting and piping.	According to local authority, customarily performed when the cylinder or vehicle is put into service, and then every 3 or 4 Years.

The general inspection is not a mandatory inspection, however the manufacturer of cylinders recommends this inspection every 3 months to ensure that the fuel storage system is in good condition. The extent of this inspection includes an examination of the following [3]:

1. Mounting System, and
2. Cylinder(s).

Inspection which relating to the installation of the CNG system is aimed at control the connection of the cylinders and equipment on the vehicle's chassis. In the case when is loosen connections of the CNG system parts it should be re-implemented process of fixing. If there is damage to the parts, make sure is it the vehicle been involved in an accident. If so, then it should be required a new certification. The inspection of the CNG cylinders is with goal to determine if there are damages. Some indicators of damage are presented in the Table 4, [3].

Table 4: Indicators of the damage on the cylinders

Cylinder Damage Type	Signs of Cylinder damage	Potential Causes of Damage
Impact	Dents, scratches, cracked or peeling laminate, crazing (hairline cracking of the laminate)	Consequent of the impact with a blunt object, or from damage when the cylinder is dropped
Cutting	Cut, scratch, gouge, peeling laminate	From a sharp or pointed object
Abrasion	Scuffs, dull or whitish appearance, flat spots	Friction between the laminate and an object in contact with the cylinder
Fire or Excessive Heat	Charred laminate, discoloration, soft spots, blistering, swelling	Direct flame, excessive heat source in contact with cylinder, excessive heat source near cylinder
Weathering	Cloudy appearance/ discoloration, soft spots	UV radiation or water impregnation through a crack in

		the laminate
Chemical Attack	Discoloration, soft spots, blistering ...	Brake fluid, any corrosive fluid

First recommendation is to regard that the cylinder is covered with an outer layer of pure epoxy resin. Due to manufacturing, thickness may vary. Cutting damage or abrasion, which is limited to this layer of pure resin, are not critical and require no damage assessment.

The Certification Inspection is a detailed examination of the mounting system and cylinder. Inspection shall be performed by trained personnel licensed in accordance with national regulations. The frequency of this inspection is designated by the local authority and is customarily performed when the cylinders or the vehicle is put into service and then at certain intervals. CNG cylinders according to UN ECE R110 have to be inspected at least every 4 years, for other cylinders; usually intervals of 3 years apply [3,12].

7.4 GENERAL RULES FOR WORKING ON CYLINDERS AND COMPONENTS

Listed below are a few important safety guidelines to follow when filling and defueling cylinders and components with pressurized natural gas [3,10].

1. Wear protective gear:
 - Safety glasses & safety boots.
2. Use correct tools:
 - Use the special tools specified by the manufacturer, if applicable, and
 - Obtain relevant documentation from the manufacturer before commencing.
3. Understand the system:
 - Only trained personnel shall perform maintenance and inspection tasks, and
 - A clear understanding of the fuel system functions is mandatory.
4. Eliminate potential ignition sources:
 - No open flame or other heat sources, and
 - Disconnect all electrical wires and ground the system to prevent sparks.
5. Assume system / component is pressurized:
 - Open fittings and ports slowly and stop immediately if gas starts to leak or if excessive torque is required to open the connection.
6. Take necessary precautions with a potentially flammable mixture:
 - Natural Gas is flammable in air at concentrations from 5% to 15%,
 - Do not operate, store or ship a system with a potentially flammable mixture. Purge the system according to relevant documentation from the manufacturer, and
 - Do not connect any electrical line to a system that contains a flammable mixture.

8. CONCLUSIONS

Use of CNG as an alternative fuel is an effective, available way to help solve environmental and fuel – resource problems. In fact, natural gas has safety advantages compared to gasoline and diesel: it is non-toxic, neither carcinogenic nor corrosive gas, and

has no potential for ground or water contamination in the event of fuel release. An odorant is added to provide a distinctive and intentionally disagreeable smell which is easy to recognize.

Substituting existing fuels by natural gas in road transport can be achieved by introducing new vehicles equipped with CNG engines, or as a first step, by converting engines of existing vehicles to CNG drive. The better variant is the using of the completely new engine with dedicated CNG combustion, which is paired with automatic gearbox and driven axle. To secure natural gas supply to the transporters and another, like the bridge before gas networking is better to use the Containers for CNG Bulk transport with truck-trailers.

CNG cylinders require an external visual re-inspection for defects in the composite wrap at certain intervals after installation or upon reinstallation. Inspection shall be in accordance with the relevant standards and regulations of the country where the cylinder is operated. According to UN ECE Regulation No. 110, the certificated inspection shall be performed at least every 48 months after the date the vehicle enters into service. General inspection performed by the driver or other service technician, is recommended every 3 months.

ACKNOWLEDGMENT

The paper is the result of the researches within the project TR 35041 financed by the Ministry of Science and Technological Development of the Republic of Serbia.

9. REFERENCES

- [1] Gas Vehicle Report: "Worldwide NGV Statistics", Int. J. of NGV group, 11#3, 124, 2012., 32-36,
- [2] Djajić, N.: "The Natural Gas – Energy Source for XXI Century", Research and design for economy, (in Serbian), 6, 22, 2008., Beograd, 49-59,
- [3] Dynetek Europe GmbH: "Fuel Storage Cylinder for the On-board Storage of CNG and Hydrogen in Vehicles", Internal document, 2009., Ratingen, 1-33,
- [4] EvoBus: "Gas bus Citaro", Internal document – presentation, 2007, Stuttgart,
- [5] Milojevic, S. and Pestic, R.: "CNG buses for clean and economical city transport", Int. J. Vehicle Mech., Engines and Transportation Syst., 37, 4, 2010., Kragujevac, 57–71,
- [6] Milojevic, S. and Pestic, R.: "Theoretical and Experimental Analysis of a CNG Cylinder Rack Connection to a Bus Roof", Int. J. Automotive Technology, 13, 3, 2012., 497-503, DOI 10.1007/s12239–012–0047–y,
- [7] Opel Special Vehicles GmbH: "Zafira 1.6 CNG monovalent^{plus} – The Natural Gas Alternative", Internal document, 2002, Russelham, 1-22,
- [8] Pešić, R., Petković, S., Hnatko, E. and Veinović, S.: "Anthropogenic global warming and renewable energy", (in Serbian), Tractors and Power Machines, 15, 2-3, 2011., Novi Sad, pp.101-108,
- [9] Pešić, R. and Milojević, S.: "The issue of control and technical inspection of vehicles at gas plant ", (in Serbian), Technical inspection of vehicles of the Serbian Republic, 2012, pp. 25-41.
- [10] Rasche, C.: "Advanced Lightweight Fuel Storage Systems TM", Dynetek Europe GmbH Presentation. <http://www.dynetek.com/pdf/AGMPresentation2009.pdf>, accessed on 18 August 2012,

- [11] South Stream Transport AG: "The South Stream Offshore Pipeline", http://www.ssttag_south-stream-offshore-pipeline-fact-sheet_5_en_20120620.pdf, accessed on 18 August 2012,
- [12] United Nations: "Specific Components of Motor Vehicles Using CNG in Their Propulsion System", UN ECE Regulation No. 110, 2008, UN, Add. 109,
- [13] Vehicle Production Rises, But Few Cars Are "Green", <http://www.worldwatch.org/node/5461>, accessed on 14.10.2011.,
- [14] Weijermars R.: "Strategy implications of world gas market dynamics", Int. J. Energy Strategy Rev.1, 2012, pp.66-70, doi:10.1016/j.esr. 2011.11.003.

¹ INVESTIGATION OF PARAMETERS AFFECTING HYDRAULIC BRAKE LOAD SENSING VALVE PERFORMANCE

Saeed Abu Alyazeed Albatlan

UDC: 629.01;62-9

Summary

Some of hydraulic brake systems for passenger cars and light trucks are provided with load sensing proportioning valve. The behavior of this valve is important to improve the braking performance. This study presents the development and validation of a mathematical model of the change of valve design parameters on its performance according to application requirements. Experiments have been performed to measure the behavior of line pressure before and after the valve. The model results have good agreement with the experimental results

Key words: Performance; Load sensing; Proportioning valve; Methods; Parameters

ISTRAŽIVANJE PARAMETARA KOJI UTIČU NA PERFORMANSE KOČNOG VENTILA OSETLJIVOG NA OPTEREĆENJE

UDC: 629.01;62-9

Rezime

Neki od hidrauličnih kočionih sistema putničkih vozila i lakih kamiona su opremljeni proporcionalnim ventilom osjetljivim na opterećenje. Poboljšanje ponašanja ovog ventila je važno u cilju poboljšanja performansi kočenja. U radu je predstavljen razvoj i validacija matematičkog modela za analizu uticaja promene projektnih parametara ventila na njegove performanse u skladu sa zahtevima primene. Eksperimenti su izvršeni za određivanje ponašanja linije pritiska ispred i iza ventila. Rezultati dobijeni modeliranjem pokazuju dobro slaganje sa eksperimentalnim rezultatima.

Ključne reči: performanse, kočni ventil osjetljiv na opterećenje, proporcionalni ventil metoda, parametri

¹ *Received September 2012, Revised: November 2012, Accepted: February 2013.*

Intentionally blank

INVESTIGATION OF PARAMETERS AFFECTING HYDRAULIC BRAKE LOAD SENSING VALVE PERFORMANCE

*Saeed Abu Alyazeed Albatlan*¹

UDC: 629.01;62-9

1. INTRODUCTION

The vehicle brake system requires performing safety under a variety of operation conditions and when the vehicle is partially or fully loaded, when braking is applied either in a straight forward or in a cornering condition. Load sensing brake proportioning valve (L.S.P.V) is a mean of proportioning the ratio of front - to - rear wheel retarding (braking) forces at the full range of vehicle loading and deceleration. It is well known that to achieve maximum deceleration or “ideal braking” the front and rear wheels should approach the locking point simultaneously. As the wheel load changes as a result of weight transfer, hence different braking force will be required to achieve the ideal braking [1-5]. Albatlan [6] presented complete models for the pressure limiting proportioning valve, link-less brake deceleration sensing valve and load-sensing proportioning valve. El Gindy et al [7] developed a mathematical model that describes the performance of a commonly used load – sensing brake proportioning valve. Khan et al [8], presented models of an analytic dynamics for vehicle brake apply system with proportioning valve. Also H. Lwai et al [9], described a link less brake deceleration sensing proportioning valve designed and developed for passenger cars and light trucks. In the brake system, it is important to reduce the rear brake pressure in order to secure the safety of the vehicle in braking. By using a L.S.P.V and electronic Load sensing brake proportioning valve (E.L.S.P.V), the L.S.P.V is a mechanical system and its brake efficiency is lower than the efficiency of E.L.S.P.V. But the cost of E.L.S.P.V is too higher so its application to the vehicle is not economical [10]. Fitting one load sensing valve for each wheel at rear and front axle improves in brake efficiency for the vehicle in its straight motion and in its cornering motion, depends on the variation of load distribution, road curvature and moving speed [11, 12]. Selecting the correct adjustable load-sensing proportioning valve for any vehicle entails not only selecting the proper point at slope limiting begins (the knee point), but also selecting the proper rate at which rear brake line pressure builds point (the slope) [13].

The aim of the present paper is to provide measures for changing valve performance according to changing its main components data and characteristics. This helps designers and users of a load sensing proportioning valve as a guide for selecting its component parameters according to their needs. Therefore; mathematical models as well as the simulation model in addition to measurements are carried out for the valve and characteristic changes are presented.

¹ Saeed Abu Alyazeed Albatlan, Higher Technological Institute, 10th of Ramadan City 6th October Branch Cairo, Egypt, Email: saeedzeed@yahoo.com

2. ACRONYMS AND NOMENCLATURE:

- D Plunger diameter (mm)
- A_D Plunger surface area (mm²)
- D_1 Rubber ring outer diameter (mm)
- A_{D1} Rubber ring surface area (mm²)
- d Plunger stem diameter (mm)
- A_d Plunger stem surface area (mm²)
- X_O Clearance between plunger and rubber ring (mm)
- Z Rubber ring deflection (mm)
- K_s Spring stiffness (N/mm)
- K_r Stiffness of the rubber ring (N/mm)
- F_{xs} Spring force (N)
- F Plunger force (N)
- P_f Front line pressure (bar)
- P_k Knee point pressure (bar)
- P_r Rear line pressure (bar)

3. THEORETICAL ANALYSIS

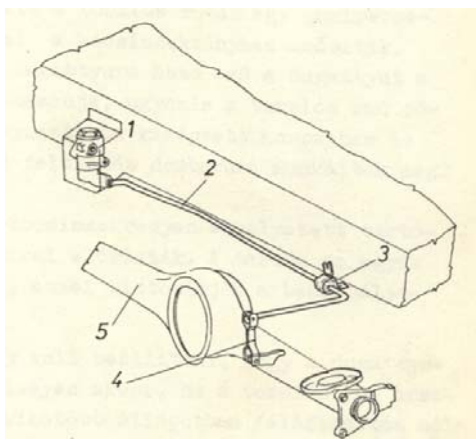
Theoretical Simulation based on the proposed mathematical models of the load-sensing proportioning valve requires that its function be represented by suitable mathematical terms. To do this, it is necessary to analyze the operation of the proportioning valve and actuating mechanism.

3.1 DESCRIPTION OF THE LOAD-SENSING PROPORTIONING VALVE (L.S.P.V).

The load-sensing proportioning valve is mounted on the rear part of the vehicle body and connected to the axle by a valve lever (torsion bar), as shown in Fig. 1. Fig. 2 shows the construction of the valve. The input line pressure P_f is equal to the line pressure of the front axle. The output line pressure P_r is a controlled pressure which is the line pressure of the rear axle. As the rear load increases the deflection increases and the twist angle of the torsion bar increases which causes an increase in the force, F acting on the end of the plunger so affecting the rear line pressure. Details of the dimensions and specifications of the valve components are shown Table 1.

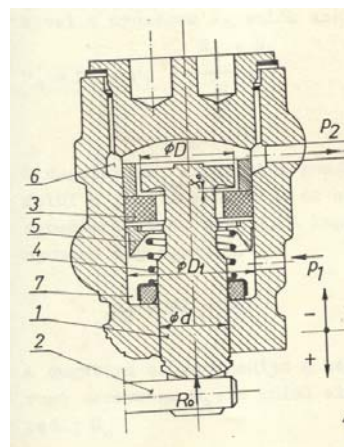
Table 1 Valve parameter values [7]

Parameter	Description	Value
D	Plunger diameter	19.0 mm
A_D	Plunger surface area	285.0 mm
D_1	Rubber ring outer diameter	25.4 mm
A_{D1}	Rubber ring surface area	507.0 mm ²
d	Plunger stem diameter	14.0 mm
A_d	Plunger stem surface area	154 mm ²
X_o	Clearance between plunger and rubber ring	0.5 mm
K_s	Spring stiffness	10.0 N/mm
K_r	Stiffness of the rubber ring	5000.0 N/mm
F_0	Force due to spring assembling	49.05 N



- 1. Load sensing proportioning valve
- 2. Torsion bar
- 3. Attached to chassis
- 4. Attached to rear axle
- 5. Rear axle

Fig. 1 Load sensing proportioning valve installation



- 1. Plunger
- 2. Torsion bar
- 3. Rubber ring
- 4. Coil spring
- 5. Coil spring cap
- 6. Valve housing

Fig. 2 Load sensing proportioning valve construction. [7]

3. 2 MATHEMATICAL MODEL

The load-sensing proportioning valve operation can be presented in two stages according to the valve plunger movement.

2.2.1 Stage (1)

The plunger should start to move downwards by a distance (X_0), at this position the plunger is in contact with rubber ring.

$$P_k = \frac{F + F_s}{A_d} \quad (1)$$

Where:

$$P_k = P_f = P_r \quad (2)$$

2.2.2 Stage (2)

Due to the continuous increase in P_f , the rubber ring is forced to be imbedded in the plunger which moves with it in the up - word direction by distance, Z , in this stage the increase of rear pressure can be determined according to:

$$P_r A_{D1} = P_f (A_{D1} - A_d) + F + F_s - Z(K_r + K_s) \quad (3)$$

$$P_r = \frac{P_f (A_{D1} - A_d) + F + F_s - Z(K_r + K_s)}{A_{D1}} \quad (4)$$

$$Z = \frac{P_f (A_{D1} - A_d) + F + F_s - P_r}{K_r + K_s} \quad (5)$$

Where:

$$F_s = X_0 K_s \quad (6)$$

Mathematical Model of the load-sensing proportioning valve constructed on Matlab (Simulink) as shown in Fig. 3. Valve data is presented in Table 1, used as inputs to the model simulation.

4. EXPERIMENTAL WORK

The objective of the experimental work is to test the load sensing proportioning valve (LSPV) under different load conditions, and to measure brake line pressure in front and rear axels. The experimental data were used for validating the mathematical model results.

The test rig was designed and constructed to simulate the vehicle hydraulic brake system. The brake apply system was set up on a test rig according to the plate shown in Fig. 4. The components to be tested include a brake pedal, tandem master cylinder, two hydraulic brakes lines connected to front calliper and rear drum with load sensing proportioning valve. The test is carried out in static manner, i.e. no dynamic loads occur. This test rig is equipped with devices in order to measure the master cylinder outlet pressure, the line pressure delivered to front (P_f) and rear wheels (P_r) by using hydraulic pressure transducers and the

pedal travel (D_2), valve plunger displacement (D_1) using position sensors. All the transducers are interfaced to a dell-500 computer, through an amplifier and signal conditions devices. The dell-500 computer is used for data acquisition and data storage. Details about this test rig are given in [6].

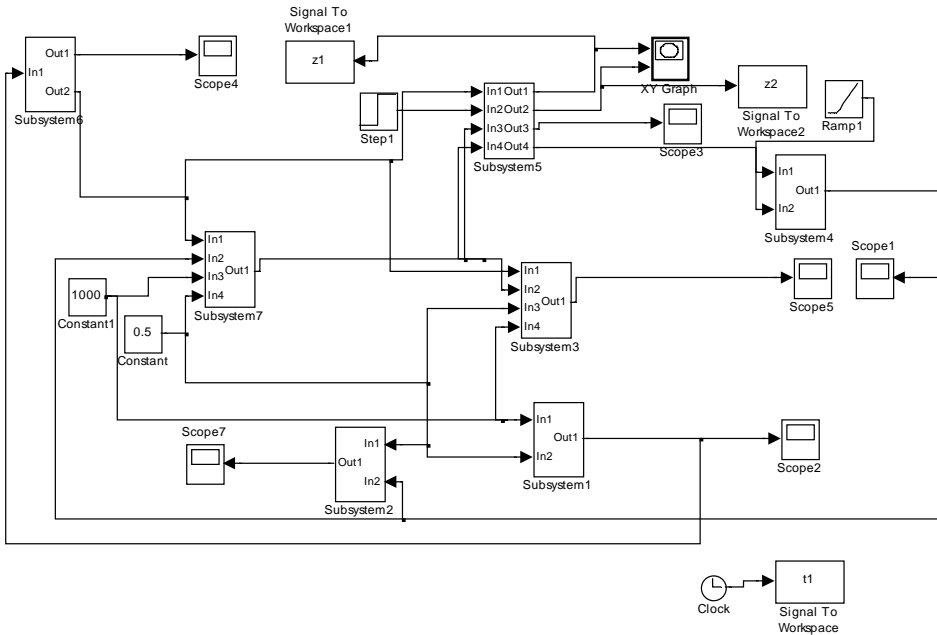
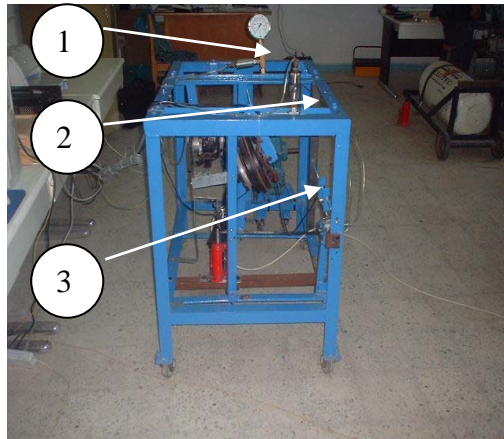


Fig.3 Valve block diagram -Simulink



1. Front pressure sensor, 2. Rear pressure sensor, 3. Load sensing proportioning valve

Fig. 3 Test rig

5. RESULTS AND DISCUSSION

This section presents validation of model simulation results. It also contains a study of the influence of valve parameters on its Performance behaviour.

5.3 MODEL VALIDATION

In order to validate this model, experimental results are compared with model simulation ones. Figs. 5 to 7 show the rear brake line pressure plotted against the front line pressure, for experimental and simulation results in different cases covering the whole loading conditions range of the vehicle.

The results show a good agreement between simulation and experimental results.

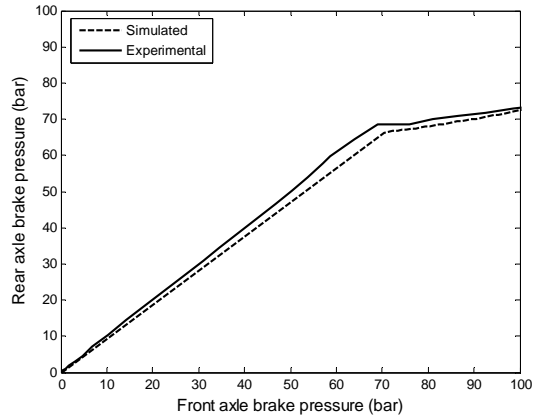


Fig. 5 Simulated and experimental for front and rear axle brake pressure

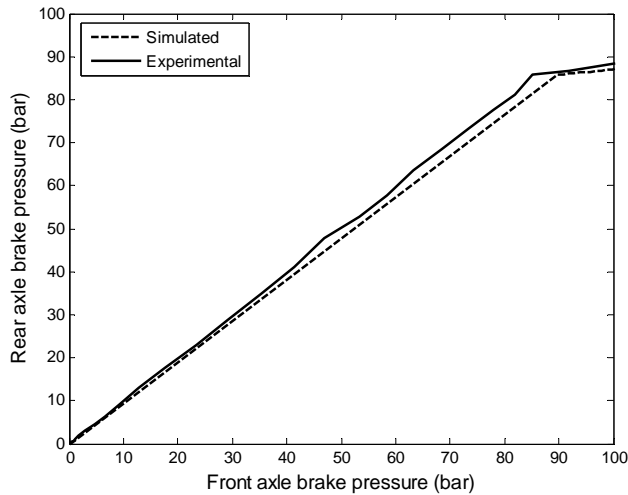


Fig. 6 Simulated and experimental for front and rear axle brake pressure

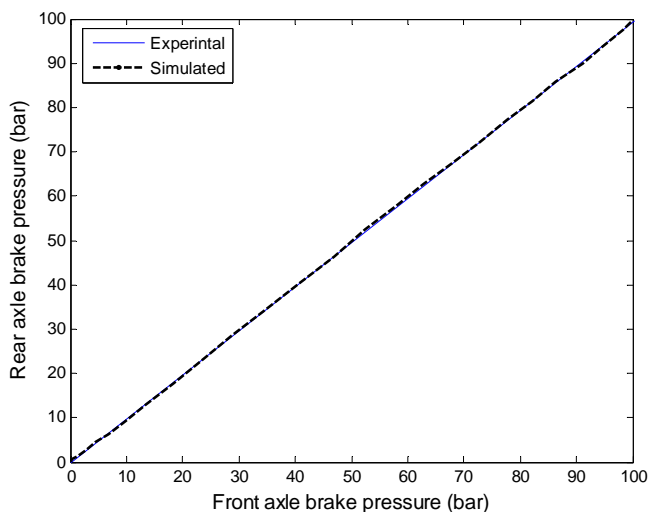


Fig. 7 Simulated and experintal for front and rear axle brake pressure

5. 4 THE INFLUENCE OF VALVE PARAMETERS ON ITS PERFORMANCE

Performance behaviour of L.S.P.V is affected by many factors, among them, the rubber ring stiffness, coil spring stiffness, clearance between plunger and rubber ring, plunger area ratio and plunger force.

The Results shown in Figs. from 8 to 14 represent the relation ship between the rear brake line pressures against the front line pressure, and indicate performance behaviour of the valve under effect of each parameter.

4. 2. 1. Effect of the rubber ring stiffness

Figure 8 compares directly between the performance behaviour of the valve at different rubber ring stiffness, 180%, 140%, 100%, 60% and 20%. The figure curves have the same knee point, but with different slopes, at lower values of rubber ring stiffness the slopes vary greater, due to increase rubber ring deflection.

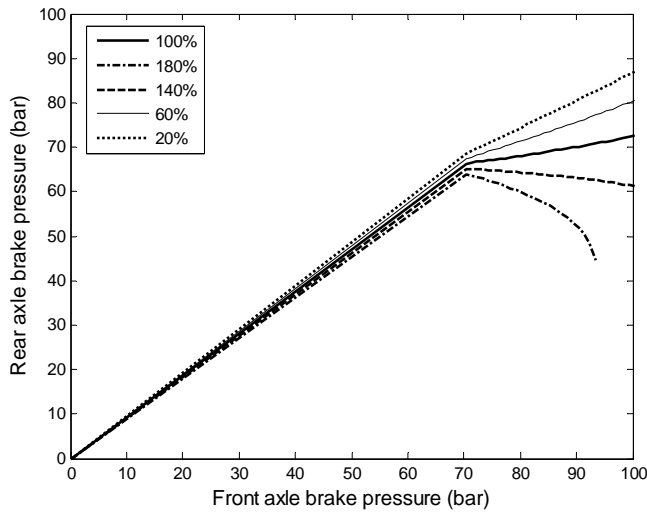


Fig. 8 Effect of rubber ring stiffness

4. 2. 2. Effect of the coil spring stiffness

Figure 9 represents the performance of valve at different ratio, 200%, 175%, 100%, 50% and 25% of coil spring stiffness. As indicated in this figure, all curves are identical; i. e. the same knee point and slopes. The effect of coil spring stiffness can be neglected.

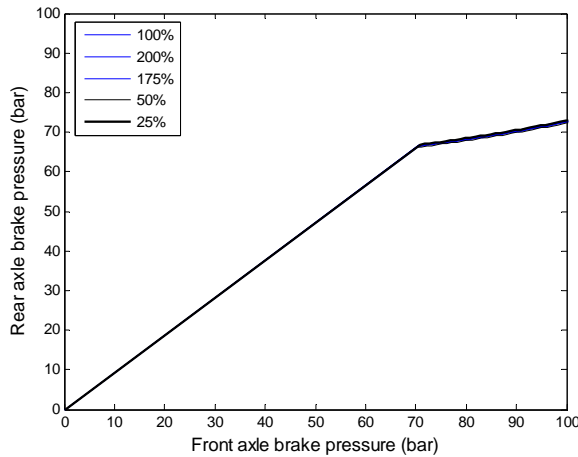


Fig. 9 Effect of coil spring stiffness

4.2.3. Effect of the clearance between plunger and rubber ring (X_0)

Figure 10 represents the performance of valve at different ratio, 250%, 200%, 150%, 100% and 50% of clearance between plunger and rubber ring. As indicated in this figure, all curves are identical; i. e. the same knee point and slopes. The effect of clearance between plunger and rubber ring can be neglected.

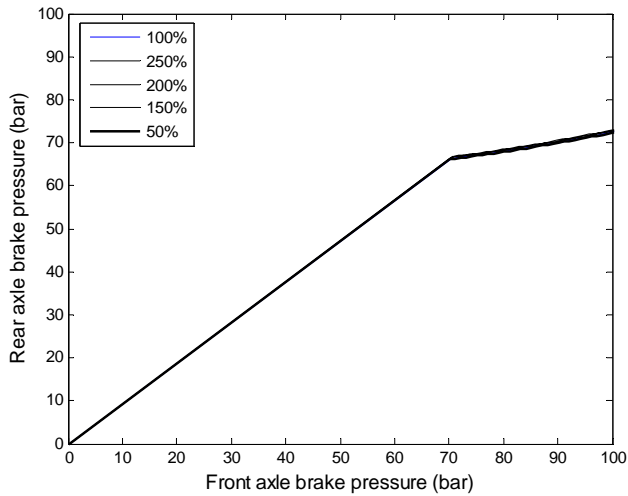


Fig. 10 Effect of clearance between plunger and rubber ring

4. 2. 4. Effect of the plunger area ratio

Figures 11 to 13 compare directly between behavior performances of the valve at different cases of area ratio.

4.2.4.1 Case (I):

Figure 11 shows values of the knee-point pressure are changed according to plunger stem surface area. The value of knee-point pressure increases clearly with lower plunger stem surface area.

4.2.4.2 Case (II):

Figure 12 shows values of the knee-point pressure increases when plunger stem surface area decreases and consequently plunger surface area increases.

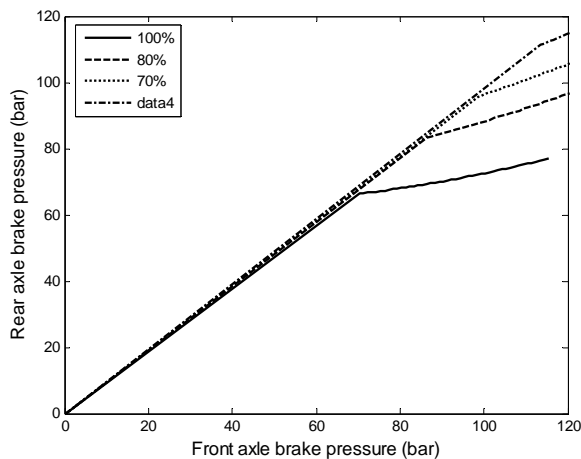


Fig. 11 Effect of plunger area ratio – Case (I)

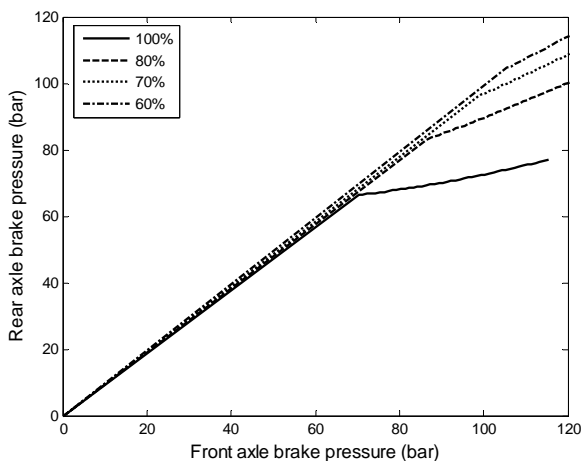


Fig. 12 Effect of plunger area ratio – Case (II)

4.2.4.3 Case (III):

Figure 13 shows values of the knee-point pressure are decreased when plunger stem surface area and plunger surface area increase.

As shown from Figs. 11 to 13, the knee point pressure changes according to area ratio and same trend of slope.

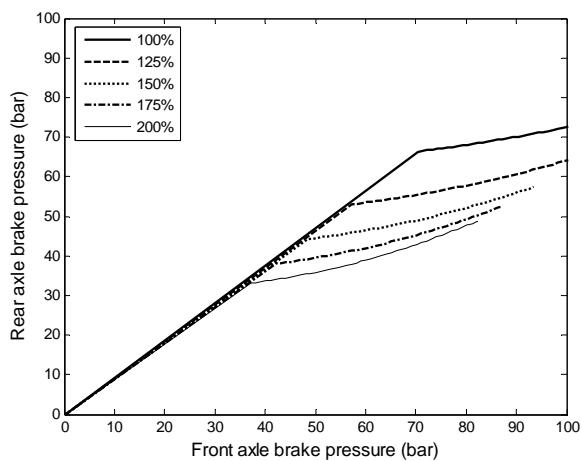


Fig. 13 Effect of plunger area ratio – Case (III)

5. 5 EFFECT OF THE PLUNGER FORCE.

Figure 14 represents the complete performance behavior at different values, 250%, 200%, 150%, 100% and 50% of plunger force. As shown from Fig. 14, the knee point pressure moves towards the higher ratio and same trend of slope.

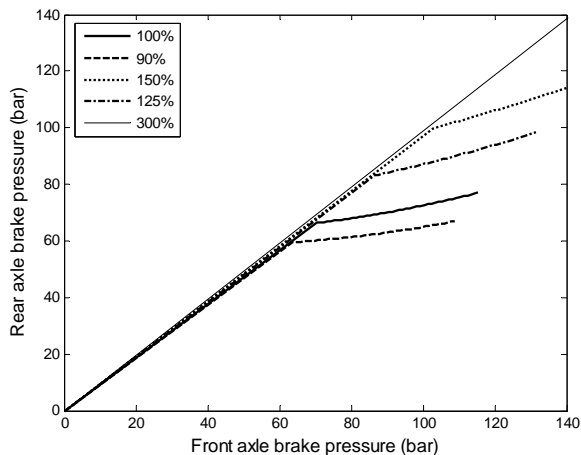


Fig. 14 Effect of plunger force

6. CONCLUSIONS

The measurements performed on the valve using a simple test rig show a good agreement with the mathematical model. Performance behaviour of load-sensing proportioning valve is affected by internal design parameters, the knee point affected by plunger area ratio and plunger force. Moreover, the slope affected by rubber ring stiffness. The effective of coil spring stiffness and clearance between plunger and rubber ring can be neglected. Selecting the correct adjustable load-sensing proportioning valve for any vehicle entails not only selecting the proper point at slope limiting begins (the knee point), but also selecting the proper rate at which rear brake line pressure builds point (the slope).

7. REFERENCES:

- [1] R.T. Eddy and R.A. Wilson, "An Approach to Load Sensing Brake Proportioning for Passenger Cars and Light Trucks." SAE. Transactions, Vol. 75 (1967), paper 660411.
- [2] Pasquale Borracci, "Proportional Braking". Automobile Engineer, Vol. 38 (October 1984). PP. 398-400.
- [3] El-Gindy, M., Saleh, M., A. and Saad, A., M., "Brake Proportioning to Load." Third A.M.E. Conference, April 1988, Cairo.
- [4] Wong, J. Y., "Theory of Ground Vehicles." John Wiley and Sons, Inc., New York 2001 (3rd ed.).
- [5] D: \ Ives\Load sensing proportioning valve for brake system - Patent 4986609. htm, 2008.
- [6] Albatlan, S. Abu Alyazeed., "Optimization of the Brake Pressure Distribution between Car Axles." M. Sc. Thesis, Ain Shams University. Faculty of Engineering. Automotive Department Cairo, 2002

- [7] El-Gindy et al, "Modeling of a Load-Sensing Brake Proportioning Valve", Third A.M.E. Conference, April 1988, Cairo.
- [8] Khan et al, "Modeling Experimentation and Simulation of a Brake Apply System", American Control Conference, June 1992.
- [9] H.. Lwai et al "Link-Less Brake Deceleration Sensing Proportioning Valve", SAE. Paper No. 810310, (1981).
- [10] Hunmo KIM, "Design of the Electronic Brake Pressure Modulator Using a Direct Adaptive Fuzzy Controller in Commercial Vehicles for The Safety of Braking in Fail." JSME International Journal, Series, C, Vol. 45, No. 1, (2002), PP. 246-257.
- [11] Nosseir et al, "Proper Utilization of Load Sensing Valve to Improve Brake Performance", Ain Shams University. Faculty of Engineering, Vol. 40, No.2, June 3 0, (2005), PP. 823-843.
- [12] Nantais Nath and Minaker Bruce P., "Active Four Wheel Brake Proportioning for Improved Performance and Safety", SAE International. Document No. 2008- 01-1224, April (2008).
- [13] Walker James, "Brake Proportioning Valves, (<http://www.teamscR.com>), (2004).

¹ COMPOSITE MATERIALS IN AUTOMOTIVE ENGINEERING – MECHANICAL BEHAVIOR OF ANISOTROPIC MEDIA

*Gordana Bogdanović, Dragan Milosavljević, Ljiljana Veljović, Aleksandar Radaković,
Mirjana Lazić*

UDC: 531/534.011.012

Summary

In recent engineering practice composite materials are widely used. In such materials two or more materials are combined to obtain a new one with new properties, while individual properties of constituents remain distinguished. Such materials have notable feature that are anisotropic, having different mechanical properties in different directions. Here is special attention devoted to their mechanical behavior. Small changes of preferred direction have significant influence to stress strain relations in fibre reinforced layers.

Fibre reinforced medium is here treated as homogeneous transversally isotropic. Here is formed *Riemann-Christoffel's equation leading to three homogeneous linear algebraic equations, from which displacements amplitudes may be determined. In such way problem may be analyzed as system of homogeneous algebraic equations.*

Developed constitutive relations are accommodated for complete analysis of dynamical behavior of plates and laminates, which is one of the basic requirement of actual technical practice.

Key words: composite materials, automotive, anisotropic media

KOMPOZITNI MATERIJALI U AUTOMOBILSKOJ INDUSTRIJI - MEHANIČKO PONAŠANJE ANIZOTROPNE SREDINE

UDC:531/534.011.012

Rezime

U savremenoj inženjerskoj praksi sve je rasprostranjenija upotreba kompozitnih materijala, kod kojih se kombinuju osobine dva ili više materijala radi dobijanja materijala sa novim karakteristikama, pri čemu se zadržavaju individualne karakteristike konstituenata. Ovi materijali imaju jednu važnu osobinu da su anizotropni, odnosno da imaju različite mehaničke osobine u različitim pravcima. U ovom radu posebna pažnja je posvećena izučavanju mehaničkog ponašanja ovih materijala. Male promene privilegovanih pravaca imaju bitan uticaj na naponsko i deformaciono polje vlaknima ojačanih slojeva.

U ovom radu je vlaknima ojačana sredina predstavljena kao homogeni, transferzalno izotropni medijum. U radu je formirana Riman Kristofelova jednačina, koja definiše tri homogene linearne jednačine, iz kojih se određuju amplitude pomeranja, kojom se problem prostiranja zapreminskih talasa svodi na sistem homogenih linearnih jednačina i predstavlja uslov propagacije.

¹ Received: January 2013, Accepted: February 2013.

Izvedene konstitutivne relacije su adaptirane za sveobuhvatnu analizu dinamičkog ponašanja ploča i laminata, što je jedan od osnovnih zahteva savremene tehničke prakse u mašinstvu.

Ključne reči: kompozitni materijali, automobilski, anizotropna sredina

COMPOSITE MATERIALS IN AUTOMOTIVE ENGINEERING – MECHANICAL BEHAVIOR OF ANISOTROPIC MEDIA

Gordana Bogdanović¹, PhD Assistant professor, Dragan Milosavljević, PhD Full professor, Ljiljana Veljović, PhD Assistant professor, Aleksandar Radaković, MSc teaching assistant, Mirjana Lazić, PhD Assistant professor

UDC:531/534.011.012

1. INTRODUCTION

Composite materials consist two or more constituents such as fibres and matrix which make layers mutually bonded to form multilayered composite called laminate. Fibres carry loads giving strength of composite, and matrix bond fibres together and have role in transfer loads to fibre, forms outer shape of composite and between other properties defines its behavior influenced by environment. Fibres are made of carbon, glass, aramid (such as kevlar) or metal, and the most often they are 60-70% of composite volume. Matrices may be made of polymers, such as thermosets or thermoplastics, metals, such as aluminum alloys or magnesium, ceramics etc.

2. GOVERNING EQUATIONS

Governing equations of elastic materials in small strain conditions are developed in the beginning of nineteenth Century. If strains are small enough equations are linear and relation connecting stress and strain are generalized Hooke's Law given as

$$\sigma_{ij} = C_{ijkl} \varepsilon_{kl} \quad (i, j, k, l = 1, 2, 3), \quad (1)$$

which is postulated by Cauchy. This law is base of linear elasticity. Coefficients C_{ijkl} are stiffness coefficients. That is tensor of fourth rank whose coefficients, in general, vary from point to point of elastic body. If these coefficients are independent on position than elastic body is homogeneous. In direct notation equation (1) may be expressed as

$$\boldsymbol{\sigma} = \mathbf{C} \boldsymbol{\varepsilon}. \quad (2)$$

Strain energy function W is specific energy of deformation and it is positive definite function. Stiffness coefficients C_{ijkl} , taking in account symmetry of stress and strain, have 21 independent components in body with general anisotropy. Strain energy W , for linear elastic materials, may be defined as quadratic in strain ε_{ij} in form

$$W = \frac{1}{2} C_{ijkl} \varepsilon_{ij} \varepsilon_{kl}, \quad (i, j, k, l = 1, 2, 3). \quad (3)$$

¹Gordana Bogdanović University of Kragujevac, Faculty of Engineering, Sestre Janjić 6, 34000 Kragujevac, Serbia, gocab@kg.ac.rs

3. LINEAR ELASTICITY – ONE FAMILY OF FIBRES

Material reinforced by one family of fibres has one preferred direction and it is transversely isotropic in relation to that direction. Preferred direction may be defined with field of unit vectors \mathbf{a} which may vary from point to point. Trajectories of unit vector field \mathbf{a} form lines called fibres and material is transversely isotropic in relation to local fibre direction. Such material is usually treated in coordinate system with one axes coincides with axes of transversal isotropy and study constrains on strain energy function from requirements that stay invariant during rotations around that axes. Here, however, we are going to use coordinate free constitutive equations following Spencer [1].

In such approach strain energy W is function of both strain $\boldsymbol{\varepsilon}$ and fibre \mathbf{a} direction, that is

$$W = W(\boldsymbol{\varepsilon}, \mathbf{a}). \quad (4)$$

The most general quadratic form of strain energy function is given as

$$W = \frac{1}{2} \lambda (tr \boldsymbol{\varepsilon})^2 + \mu_T tr \boldsymbol{\varepsilon}^2 + \alpha (\mathbf{a} \cdot \boldsymbol{\varepsilon} \cdot \mathbf{a}) tr \boldsymbol{\varepsilon} + 2(\mu_L - \mu_T) \mathbf{a} \cdot \boldsymbol{\varepsilon}^2 \cdot \mathbf{a} + \frac{1}{2} \beta (\mathbf{a} \cdot \boldsymbol{\varepsilon} \cdot \mathbf{a})^2, \quad (5)$$

where $\lambda, \mu_T, \mu_L, \alpha, \beta$ represent elastic constants.

Constitutive relation then may be expressed as

$$\sigma_{ij} = \frac{\partial W}{\partial \varepsilon_{ij}} = \lambda \varepsilon_{rr} \delta_{ij} + 2\mu_T \varepsilon_{ij} + 2(\mu_L - \mu_T) (a_i \varepsilon_{jn} a_n + a_n \varepsilon_{ni} a_j) + \alpha (\varepsilon_{rr} a_i a_j + a_m \varepsilon_{mn} a_n \delta_{ij}) + \beta (a_m \varepsilon_{mn} a_n) a_i a_j. \quad (6)$$

Stiffness tensor then may be calculated, as shown in [2], in following way

$$C_{ijkl} = \frac{\partial^2 W}{\partial \varepsilon_{ij} \partial \varepsilon_{kl}} = \lambda \delta_{ij} \delta_{kl} + \mu_T (\delta_{ik} \delta_{jl} + \delta_{jk} \delta_{il}) + (\mu_L - \mu_T) (a_i a_k \delta_{jl} + a_i a_l \delta_{jk} + a_j a_k \delta_{il} + a_j a_l \delta_{ik}) + \alpha (a_k a_l \delta_{ij} + a_i a_j \delta_{kl}) + \beta a_i a_j a_k a_l, \quad (7)$$

showing obvious dependence on fibre direction.

Expression (7) is in agreement with well known expressions for transversally isotropic linear elastic material. Stiffness coefficients may be expressed in relation to other engineering constants more suitable for direct measuring. Material constant μ_L represents shear modulus along the fibre direction \mathbf{a} , while μ_T represents shear modulus perpendicular to the fibre direction \mathbf{a} . Remained material constants λ, α, β may be connected to other modulus such as extension modulus, Yung's modulus or Poisson ratio.

Taking fibre direction to be along axes x_1 of Cartesian coordinate system leads to expression of unit fibre direction vector $(a_i) = (a_1, 0, 0) = (1, 0, 0)$ and using Voight notation in (7) one obtains

$$\begin{aligned}
 C_{11} &= \lambda + 2\alpha + \beta + 4\mu_L - 2\mu_T, \\
 C_{12} &= \lambda + \alpha = C_{21}, \\
 C_{13} &= \lambda + \alpha = C_{31}, \\
 C_{22} &= \lambda + 2\mu_T, \\
 C_{23} &= \lambda = C_{32}, \\
 C_{33} &= \lambda + 2\mu_T, \\
 C_{44} &= \mu_T, \\
 C_{55} &= \mu_L, \\
 C_{66} &= \mu_L,
 \end{aligned} \tag{8}$$

and all remained constants vanish, that is

$$C_{14} = C_{15} = C_{16} = C_{24} = C_{25} = C_{26} = C_{34} = C_{35} = C_{36} = C_{45} = C_{46} = C_{56} = 0. \tag{9}$$

In Voight notation indices 11, 22 and 33 take values 1, 2 and 3, respectively, and indices 23, 13 and 12 take values 4, 5 and 6, respectively.

4. BULK WAVES

Mechanical behavior of anisotropic media may be seen through examination of bulk waves. These waves propagate through unbounded media without perturbations caused by boundaries and inter layers. Bulk waves may be decomposed in finite plane waves which propagate along arbitrary direction \mathbf{n} inside solid.

Properties of these waves, according to [3], are determined with propagation direction and constitutive properties of media. In general, it is possible to generate three types of such waves, which are determined with three displacement vectors $\mathbf{U}^{(k)}$, $k = 1, 2, 3$ representing acoustical polarization. These polarization vectors, with propagation directions, are shown in sketch in Figure 1. Three polarization vectors are mutually orthogonal, but usually any of them are neither parallel nor perpendicular to propagation direction \mathbf{n} .

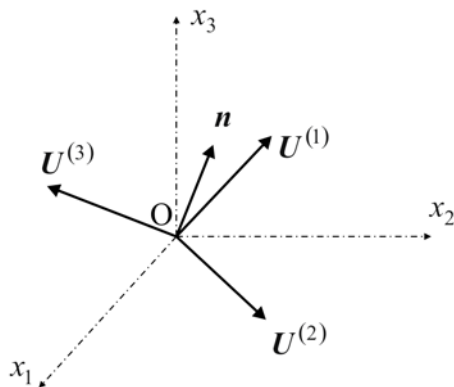


Figure 1 Typical scheme of polarization in anisotropic media

In anisotropic media “pure” modes may appear for some particular propagation directions only, depending on degree of symmetry of considered material.

3.1 Propagation conditions

Propagation of elastic waves may be examined according to first Cauchy law of motion. Taking fact that stiffness tensor C_{ijkl} possess symmetry in relation to second pair of indices one may write equations

$$\rho \frac{\partial^2 u_i}{\partial t^2} = C_{ijkl} \frac{\partial^2 u_l}{\partial x_j \partial x_k}, \quad (10)$$

which represent system of homogeneous linear differential equations of second order in relation to displacement vectors. Solution of such system of equations may be supposed as plain wave solution with wave normal with components $(n_i) = (n_1, n_2, n_3)$ with displacement vector given as

$$u_i = U_i e^{i(kn_j x_j - \omega t)} = U_i e^{i\varphi} \quad (11)$$

Expression (11) gives complex displacement, although displacement should be real. Vector (11) will satisfy system of homogeneous linear differential equations (10) if both real and imaginary parts satisfy (11). Substituting (11) in (10), taking into account $\partial u_i / \partial x_j = i k n_j u_i$, leads to

$$(C_{ijkl} n_k n_j - \rho v^2 \delta_{il}) U_l = 0 \quad (12)$$

Second order tensor Λ_{il} , introducing $\lambda_{ijkl} = C_{ijkl} / \rho$, which may be expressed as

$$\Lambda_{il} = \lambda_{ijkl} n_k n_j \quad (13)$$

is called Riemann-Christoffel's tensor, and equation (13) may be written as

$$(\Lambda_{il} - v^2 \delta_{il}) U_l = 0. \quad (14)$$

This equation is known as Riemann-Christoffel’s equation and represents system of three homogeneous linear equations in relation to displacement amplitudes U_l . Equation (14) in matrix form is

$$\begin{bmatrix} \Lambda_{11} - v^2 & \Lambda_{12} & \Lambda_{13} \\ \Lambda_{12} & \Lambda_{22} - v^2 & \Lambda_{23} \\ \Lambda_{13} & \Lambda_{23} & \Lambda_{33} - v^2 \end{bmatrix} \begin{Bmatrix} U_1 \\ U_2 \\ U_3 \end{Bmatrix} = 0, \tag{15}$$

where elements Λ_{il} , using relation (13), may be expressed in the following way

$$\rho\Lambda_{il} = C_{ijkl}n_k n_j = C_{i11l}n_1 n_1 + (C_{i12l} + C_{i21l})n_1 n_2 + (C_{i13l} + C_{i31l})n_1 n_3 + C_{i22l}n_2 n_2 + (C_{i23l} + C_{i32l})n_2 n_3 + C_{i33l}n_3 n_3. \tag{16}$$

5. NUMERICAL EVALUATION OF SLOWNESS SURFACES

Materials reinforced by one family of fibres possess transversal isotropy and, without loss of generality, one may choose one of Cartesian axis, say x_1 , to coincide with fibre direction. Thus, unit vector of fibre direction may be written as $(a_i) = (1, 0, 0)$, and components of acoustic tensor (16), with use of (8), may be expressed as

$$\begin{aligned} \rho\Lambda_{11} &= (\lambda + 2\alpha + \beta + 4\mu_L - 2\mu_T)n_1^2 + \mu_L n_2^2 + \mu_L n_3^2, \\ \rho\Lambda_{12} &= (\lambda + \alpha + \mu_L)n_1 n_2, \\ \rho\Lambda_{13} &= (\lambda + \alpha + \mu_L)n_1 n_3, \\ \rho\Lambda_{22} &= \mu_L n_1^2 + (\lambda + 2\mu_T)n_2^2 + \mu_T n_3^2, \\ \rho\Lambda_{23} &= (\lambda + \mu_T)n_2 n_3, \\ \rho\Lambda_{33} &= \mu_L n_1^2 + \mu_T n_2^2 + (\lambda + 2\mu_T)n_3^2. \end{aligned} \tag{17}$$

Let suppose that propagation direction is in coordinate plane (x_1, x_3) , then wave normal vector is $(n_i) = (n_1, 0, n_3)$, and in (17) Λ_{12} and Λ_{23} vanish leading to

$$\begin{bmatrix} \Lambda_{11} - v^2 & 0 & \Lambda_{13} \\ 0 & \Lambda_{22} - v^2 & 0 \\ \Lambda_{13} & 0 & \Lambda_{33} - v^2 \end{bmatrix} \begin{Bmatrix} U_1 \\ U_2 \\ U_3 \end{Bmatrix} = 0 \tag{18}$$

Riemann-Christoffel’s equation may be solved analytically for very simple material symmetries only. In general, it is necessary to calculate wave surfaces numerically. Having in mind that crystallographic axes are known the simplest way of calculation is to coincide axes of symmetry with coordinate axes.

Let us choose Cartesian system (ξ_1, ξ_2, ξ_3) whose axes coincide with axes of material symmetries. We may imagine vertical plane, which coincide initially with coordinate plane (ξ_1, ξ_3) and rotate around vertical axis ξ_3 for arbitrary angle θ . That plane is referred as sagittal plane. To simplify analysis and calculations it is useful to consider slowness surfaces, representing inversed velocities. These surfaces may be obtained by calculating phase velocities for chosen propagation direction, and then calculating of slowness as inverse of phase velocity. Slowness then may be drawn as function of propagation direction.

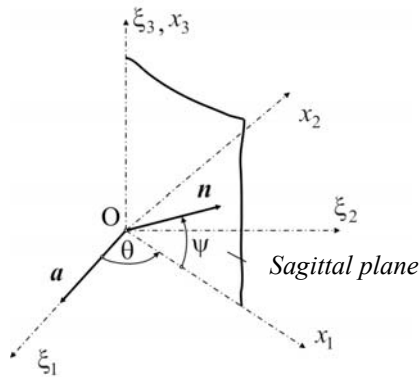


Figure 2 One family of fibres

In slowness surface is curved line, as intersection of slowness surface and sagittal plane, and each calculation leads to one point of all quasi-longitudinal and two quasi-transversal slowness curves. By choosing propagation direction to be in sagittal plane and adding certain increment to angle of wave normal to horizontal axes it may be drawn complete slowness curve in sagittal plane. Rotation of sagittal plane around vertical x_3 axes, for certain increment, one may obtain complete slowness surface for all three waves. That is illustrates in figure 2.

Slowness curves in sagittal plane, in general are three closed curves which may intersect each other. Two slower wave speeds, represented with outer curves are quasi shear curves. Depending on material symmetry these curves may intersect each other or, in case of isotropic material, to coincide. On the contrary, inner slowness curve, which is separated of other two, is convex and represents quasi-longitudinal waves which travel with highest speed.

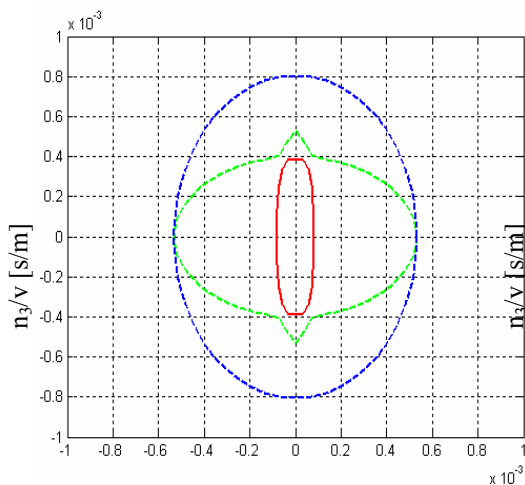
For numerical calculation is employed carbon fibre epoxy resin composite which represents strongly anisotropic material. Material constants, for such materials are measured by ultrasound methods and reported in [4], have values

$$\begin{aligned} \lambda &= 5,65 \cdot 10^9 \text{ Nm}^{-2}, \quad \mu_T = 2,46 \cdot 10^9 \text{ Nm}^{-2}, \quad \mu_L = 5,66 \cdot 10^9 \text{ Nm}^{-2}, \\ \alpha &= -1,28 \cdot 10^9 \text{ Nm}^{-2}, \quad \beta = 220,90 \cdot 10^9 \text{ Nm}^{-2}, \end{aligned} \quad (19)$$

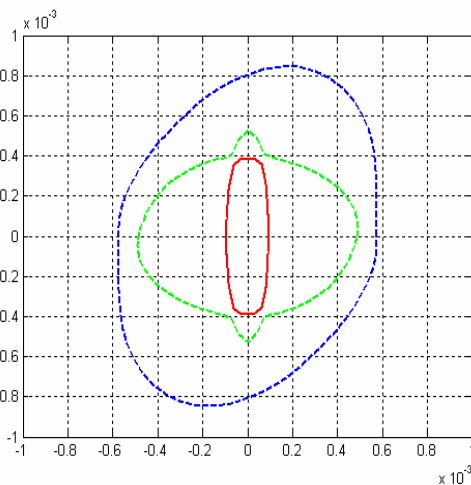
where as density is given as $\rho = 1,60 \cdot 10^3 \text{ kg / m}^3$.

By varying angle ψ between 0 and 2π may be calculated slowness curve in sagittal plane whereas by rotating of sagittal plane around axes x_3 for angle θ slowness surface may be completed. Slowness surfaces, for material reinforced by one family of fibres, are calculated in program pack MATLAB and presented in figures 3 to 6, for angles θ varies as $0^0, 30^0, 45^0$ and 90^0 , respectively. In these figures quasi-longitudinal waves are represented with solid lines, whereas quasi-transversal waves are represented with broken lines.

In figure 3, for $\theta = 0^0$, sagittal plane contains axis ξ_1 , which coincide with axis x_1 , and, therefore coincide with preferred direction, that is with fibre direction. All three modes are clearly distinguished in sagittal plane except when propagating direction is along x_1 axis, for $\psi = 0^0$, in which case two quasi-transversal waves have same speed, that is they meet each other. That is clear considering that propagation direction is along fibre direction and in plane perpendicular to fibres material behaves as isotropic.



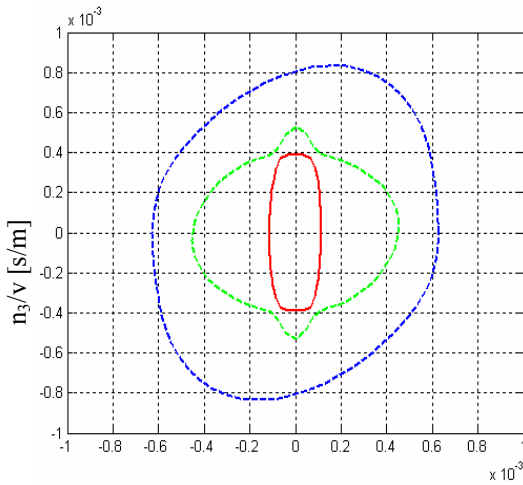
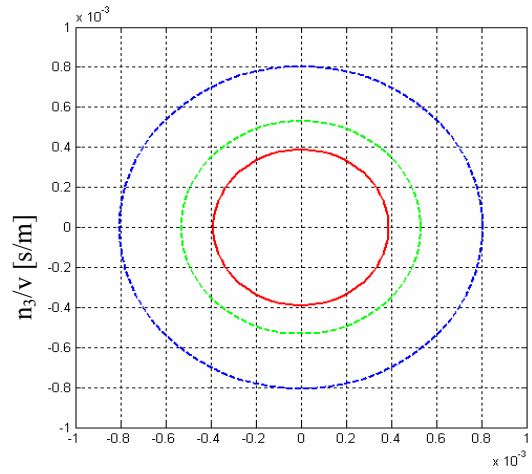
n_1/v [s/m]



n_1/v [s/m]

Figure 3 One family of fibres $\theta = 0^0$

Figure 4 One family of fibres $\theta = 30^0$

 n_1/v [s/m] n_1/v [s/m]**Figure 5** One family of fibres $\theta = 45^\circ$ **Figure 6** One family of fibres $\theta = 90^\circ$

Increasing of sagittal plane rotation angle implies, as may be noticed in figures 4, $\theta = 30^\circ$ and 5, $\theta = 45^\circ$, that slowness curve of quasi-longitudinal wave have elliptic shape, whereas quasi-transversal waves behave in such way that “faster” wave deviate from elliptic shape in regions in which propagation direction approaches to normal to fibre.

For sagittal plane angle, $\theta = 90^\circ$, as shown in figure 6, wave propagates normal to fibre and fibres are “embedded” in wave surface and, therefore one may observe three “pure” modes along symmetry lines, which propagate with constant intensity speeds, which may be concluded from the fact that slowness curves are circular.

6. CONCLUSIONS

Mechanics of continuum treats material on macroscopic level in which microscopic level may be used as preparation for homogenization purposes. Anisotropy has different effects on wave propagation as well as on complete elastic behavior of media, which may be observed through fact that wave front deviate from spherical shape. General conclusions about anisotropic material behavior, in mechanical sense, are taken from considering of bulk waves propagation.

For considered material acoustic tensor, as propagation condition, has been formed, and determined for different directions of wave propagation. For particular material reinforced by one family of fibres components of that tensor are calculated.

These calculations has practical significance, because it has been formed easy mathematical approach which may give fast answer about material behavior in dynamic circumstances, which often appear in parts of motor vehicles.

This approach may be used as first approximation of dynamical behavior of real parts with anisotropic characteristics that appears very often in consideration of vehicle construction parts.

ACKNOWLEDGMENTS

This investigation is a part of the project TR 33015 of Technological Development of the Republic of Serbia. We would like to thank to the Ministry of Education and Science of Republic of Serbia for the financial support during this investigation.

7. REFERENCES

- [1] Spencer, A.J.M.: “Formulation of constitutive equations for anisotropic solids”, *Mechanical Behaviour of Anisotropic Solids*, J.P. Boehler eds., 1982, Amsterdam, 3-26,
- [2] Milosavljević, D., Bogdanović G., Veljović, L.J., Radaković, A., Lazić, M.: “Failure criteria of fibre reinforced composites in homogenous temperature field”, *International Journal Thermal Science*, Vol. 14 suppl., 2010. S285-S297,
- [3] Nayfeh, A.H.: “Wave Propagation in Layered anisotropic Media”, Elsevier, 1995
- [4] Markham, M., F.: “Measurement of the Elastic Constant of Fibre Composites by Ultrasonics”, *Composites*, 1, pp. 145-149, 1970.
- [5] Bogdanovic, G.: “Dynamical behavior of composite laminates”, Ph.D Thesis, Kragujevac, 2011.

Intentionally blank

¹THE INFLUENCE OF VARIATION IN POSITION OF OUTPUT SHAFT TO LOAD ON THE CARDAN JOINT CROSS SHAFT

Boris Rakić, Lozica Ivanović, Danica Josifović, Blaža Stojanović, Andreja Ilić

UDC: 621.825

Summary

In this paper, the analysis of the influence of variation in position of output shaft to load on the Cardan joint cross shaft in power transmitters is shown. Cardan shafts are the systems that provide alterations of angles between axes of the shafts, which are involved in the power transmission, so as their relative translations. Those properties make Cardan shafts very suitable for using in power transmitters, especially at motor vehicles. The kinematic of power transmitters with Cardan joints is highly specific in relation to variation in position of the axis of the output and input shafts. Those variations in positions cause the alterations of the maximal stresses at the branches of the Cardan joint cross shaft and, also, at its bases. The analysis of the motions at this power transmitter is presented in the first part of the paper and also, the diagrams of relations between the specific kinematic values are given. The analytical calculation of the stresses at the cross shaft of the Cardan joint, as function of the angular position of the shaft is done. The second part of the paper deals with forming of the analytic, so as with numeric calculation of stresses in the critical section of the cross shaft. The results obtained by numeric and analytic method are evaluated and the conclusions about stress concentration and stress distribution for different positions of Cardan joints are done.

Key words: Cardan joint, cross shaft, kinematic analysis, critical stress level, numeric method

UTICAJ PROMENE POLOŽAJA GONJENOG VRATILA NA OPTEREĆENJE KRSTASTE OSOVINE KARDANSKOG PRENOSNIKA

UDC: 621.825

Rezime

U radu je prikazana analiza uticaja promene položaja gonjenog vratila na opterećenje krstaste osovine kardanskog prenosnika. Kardansko vratilo je sistem koji omogućava naginjanje, a i translaciju ose vratila kojim se prenosi snaga, što ga čini veoma pogodnim za prenos snage, pre svega kod motornih vozila. Kinematika kardanskih prenosnika je vrlo specifična s obzirom na promenu položaja ose gonjenog u odnosu na osu pogonskog vratila, što se odražava na promenu maksimalnih napona na rukavcu krstaste osovine i u njegovom korenu. U prvom delu radu analizirano je kretanje ovog prenosnika i dat je dijagramski prikaz međusobnih zavisnosti pojedinih kinematskih veličina. Izveden je analitički proračun napona na krstastoj osovini u zavisnosti od ugaonog položaja vratila. Drugi deo rada se

¹*Received: January 2013, Accepted: February 2013.*

odnosi na formiranje numeričkog modela, kao i numeričkog proračuna napona u kritičnom preseku krstaste osovine. Analizirani su rezultati dobijeni numeričkom i analitičkom metodom i izvedeni zaključci o koncentraciji i raspodeli napona u različitim položajima kardanskog vratila.

Ključne reči: Kardansko vratilo, krstasta osovina, kinematska analiza, kritični napon, numerička metoda

THE INFLUENCE OF VARIATION IN POSITION OF OUTPUT SHAFT TO LOAD ON THE CARDAN JOINT CROSS SHAFT

Boris Rakić¹, Master student, Lozica Ivanović, Associate professor, Danica Josifović, Full professor, Blaža Stojanović, Assistant, Andreja Ilić, PhD Student

UDC: 621.825

INTRODUCTION

Fast development of Cardan mechanisms and their' even wider usage are implicated by development of agricultural and transport mechanical engineering. The area of Cardan mechanisms usage, its exploitation properties, reliability and function ability in different exploitation conditions are determined by its constructional characteristics. Cardan mechanisms are used in many area of mechanical engineering as mechanical power transmitters, and its general classification is done on the constructional possibilities of torque transmitting. In present mechanical construction, the Cardan mechanisms with cross shaft is commonly used [11]. At tractors and other working machines, the Cardan shaft is used for transmission of power from the engine to the devices that are not rigidly connected with the engine (additional devices, tractor trailer, ...) for connecting shaft. Cardan transmitters are widely used at agricultural equipment due to possibility of continual changing of relative position of shafts in transmitter mechanism in exploitation caused by changing of terrain and characteristics of technological process. The present researches of Cardan shafts are focused on improvement of its reliability in exploitation at agricultural equipment that works in even harder conditions.

The causes of failures and design of power transmitters with Cardan shafts are analyzed by many researches. Hummel and Chassapis [2] researched on the design of the universal joints. They give some suggestions on the configuration design and optimization of universal joints with manufacturing tolerances [3]. Bayrakceken et al. [1] performed the fracture analysis of a universal joint yoke and a drive shaft of an automobile power transmission system. Spectroscopic analyses, metallographic analyses and hardness measurements are carried out for each part. For the determination of stress conditions at the failed section, stress analyses are also carried out by the finite element method (FEM). The reference [8] considered modification of design of Cardan shaft in order to avoid failures during exploitation period. The modifications of designs are analyzed by finite elements methods and the best modification of design with decrease of dimensions of input Cardan joint yoke is identified.

For the rational design, safety and reliability evaluations of machines' elements it is necessary to determine the stress levels and its distributions in the critical zones. The stress level and its distributions depend on load characteristics so as on the shape of the machines' elements. At the zones with variation in shape and dimensions of cross section the stresses are irregularly distributed and the maximal stresses are far greater than nominal stresses. Besides that, the multiple stress concentrations as the consequence of multiple stresses concentrators influence are induced [6]. For the aim of reducing the stress concentration the design and technological procedures are done. By the increase of fillets at critical zones, the

¹ Boris Rakić, Master student, Faculty of Engineering, Sestre Janjić 6, 34000 Kragujevac, Serbia, e-mail: borisrmfkg@gmail.com

stress concentrations can be significantly reduced. But, the possibilities of this procedure are limited due to interferes with axial support of bearings. In the paper [5] the procedure of identification of optimal combination of shape and dimensions of shape transition zones from the aspects of maximal stresses reductions is shown.

By the analysis of information and data obtained in many researches related to this area referred the fact that exploitation reliability of Cardan shaft in working machines are directly determined primary by reliability of needle bearing and cross shafts. Roller bearings and cross shafts work in very hard conditions because in exploitation high impacts loads are provoked. The main causes of high impact loads are inhomogeneity of ground and variation on operation angles due to agri-technical condition in which agriculture equipment is used. In those causes operation angle can overcome the defined limit. In the cause when Cardan shafts worked with high operating angles the increase of inertial forces are induced that act on roller bearings and Cardan shaft with external load. This processes lead to severe damages of roller bearings and cross shafts that have failure and breakage of Cardan shaft, as consequence. To the aim the better understanding of possibilities of improves the reliability of working machines the object of research that is presented in this paper, is the analysis of the influence of variation in position of output shaft to load on the Cardan joint cross shaft.

1. KINEMATIC OF CARDAN MECHANISMS

A universal joint is a positive, mechanical connection between rotating shafts, which are usually not parallel, but intersecting. They are used to transmit motion, power or both.

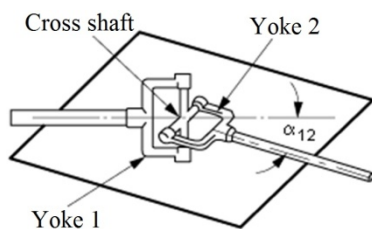


Figure 1: Single Cardan joint [12]

The simplest and most common type is called Cardan joint or Hooke joint. It is shown at Figure 1 and it consists of two yokes, one on each shaft, connected by a cross-shaped intermediate member called the cross shaft. The angle between the two shafts is called the operating angle and it is, in general, but not necessary, constant during operation. Good design practice requires low operation angles, often less than 25° , depending on the application. Independent of this guideline, mechanical interference in the construction of Cardan joints limits the operating angle to a maximum value that depends on its proportions.

The main property of the Cardan mechanisms is possibility of changing the rotation speed ratio. Amplitude of periodical variation of rotation speed ratio depends on value of the angle between input and output shafts [10], [11]. The relation between the rotation angles of input and output shafts is function of their' relative positions in the area.

Independently of types and constructional solutions of Cardan mechanisms the basic kinematic relations are equivalent. The Cardan mechanism with angle α_{12} between

shafts is presented at Fig. 1. If the rotation angle of input shaft is φ_1 then rotation angle of the output shaft is φ_2 . The relation between those angles presents the basic kinematic principle that is given in the following form [11]:

$$\varphi_2 = \arctg\left(\frac{\operatorname{tg}\varphi_1}{\cos\alpha_{12}}\right). \tag{1}$$

The difference in value of angles φ_1 and φ_2 implicate the difference in rotational speeds of the corresponding shafts ($\omega_1=d\varphi_1/dt$, $\omega_2=d\varphi_2/dt$) and the value of that difference in rotational speeds can be obtained by differentiation of the equation (1). By applying certain trigonometrical transformation the relation for rotation speed ratio of Cardan mechanism can be obtained [11]:

$$i_{21} = \frac{\omega_2}{\omega_1} = \frac{\cos\alpha_{12}}{1 - \sin^2\alpha_{12}\cos^2\varphi_1}. \tag{2}$$

Diagram of relations between certain kinematic parameters at Cardan mechanism is presented at Fig. 2, Fig. 3 and Fig. 4.

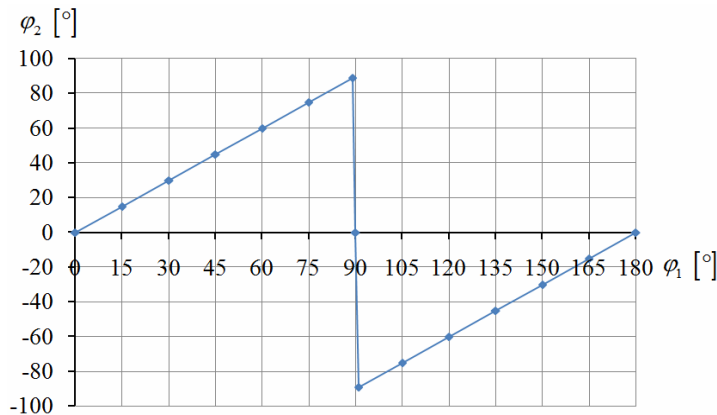


Figure 2: The relations between the rotation angles of shafts at Cardan joint

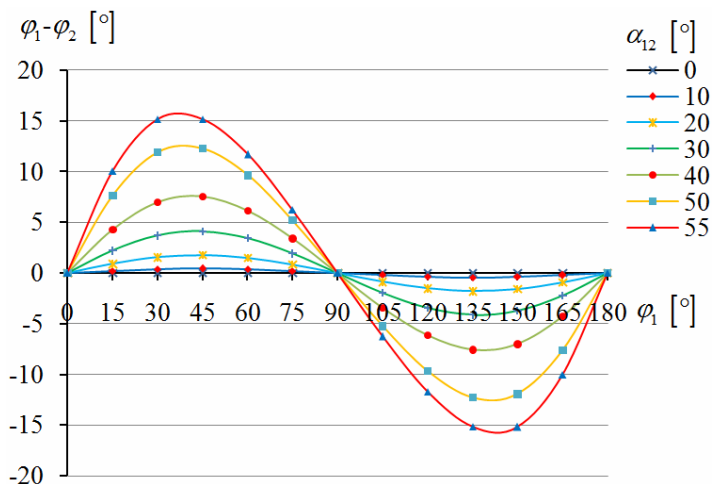


Figure 3: The difference of rotation angles of input and output shafts at Cardan joint

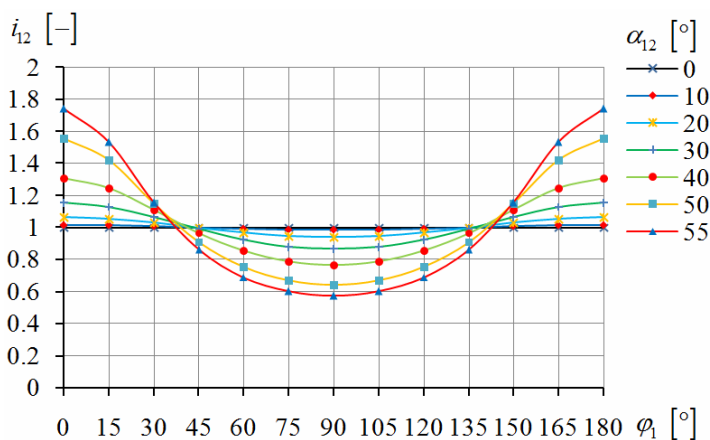


Figure 4: Ratio between the angular velocities $i_{21} = \omega_2/\omega_1$

2. CALCULATION OF STRESSES ON CARDAN JOINT CROSS SHAFT AT DIFFERENT ROTATION ANGLES

The elements of Cardan joint are loaded by complex loads on flexion, torsion, shear and surface pressure. The different phenomena of failures in material can be induced in exploitation due to overload that could lead to damages and breakages of Cardan joint elements. The usual zones in which those failures occurred are zones at the basis of branches of the Cardan joint yoke. The initial cracks as causes of failures often started on the cross shaft in the zone of hole below the lubrication spot. Kinematic of power transmitters with Cardan joints is very specific from the aspect of variation in relative positions of input and output shafts that cause the variation of maximal stresses at branches and central zone of the cross shaft.

2.1 Calculation of stresses by analytic method

The research presented in the paper [5] implicate that maximal stresses at the basis of the branches of the cross shaft can be significantly reduced by modifications of shape and fillet at the zones of shape transitions. The conducted research implicate that optimal design solution of shape transition zone from the central part to the branches is one with bigger level of fillet and chamfer with angle less of 45° to the cylindrical part for the base of needle bearing. The calculation of stresses by analytic method is done for the design of cross shaft, presented at Fig. 5. The dimensions of considered model are limited by construction requirements. The basic properties of considered power transmitter with Cardan joint are: power $P=25$ kW, number of rotation $n=1500$ min⁻¹, distance between top of branches and critical cross section $h_1=21.5$ mm, the length of bearing zone $h_2=17.5$ mm, distance between two top sides of opposite branches $L=70$ mm, diameter of branches $d=18$ mm, diameter of hole for supply of lubricant $d_1=4$ mm, the angle between input and output Cardan joint yokes is $\alpha_{12}=(0\div55^\circ)$.

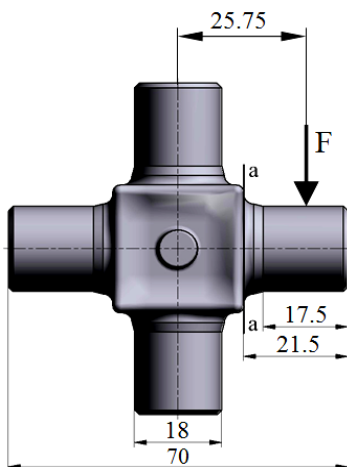


Figure 5: Dimensions and shape of cross shaft

The determined value of stress presents the maximal value of stress at critical cross section. This value is not determined for the real shape of cross shaft that enclose the presence of stress concentrators, so for determination of stresses at real model of cross shaft the numerical method must be used. From the aspect that cross shafts can be made of different steel grades, some data obtained in exploitation indicate that it is beneficial if bending stress do not exceed 150 MPa [11]. The torsion torque on input shaft T_{u1} is in equivalence with torsion torque T_{u2} on output shaft. For determination on value of the torque T_{u2} at current position of Cardan mechanism defined by rotation angle φ_1 , the method of possible movements is used. According to this method the result of actions of all elementary actions of active forces that act on the system during any possible movement is equal to zero [11]. For the static equivalence, the following relation must be satisfied:

$$T_{u1}d\varphi_1 - T_{u2}d\varphi_2 = 0. \tag{3}$$

On the basis of the assume that support bearings are rigid, the possible movement of the shafts 1 and 2 are only rotation defined by elementary angles $d\varphi_1$ and $d\varphi_2$. The relation between angles φ_1 and φ_2 is presented by equitation (1). By the transformation of the equitation (1) and using the equitation for static equivalence the torsion torque on output shaft can be determined in the following form:

$$T_{u2} = T_{u1} \frac{\cos^2 \varphi_1 \cos^2 \alpha_{12} + \sin^2 \varphi_1}{\cos \alpha_{12}}, \quad (4)$$

while maximal force on branch of the cross shaft can be determined as:

$$F = \frac{T_{u2\max}}{L - h_2}. \quad (5)$$

The stress due to flexion at the basis of the branches of the cross shafts (critical cross section a-a, presented at Fig. 5) can be determined by following relation:

$$\sigma_s = \frac{32 \cdot T_{u2\max} \cdot \left(h_1 - \frac{h_2}{2} \right)}{(L - h_2) \cdot \pi \cdot (d^3 - d_1^3)}, \quad (6)$$

while shear stress can be determined by relation:

$$\tau = \frac{4 \cdot F}{\pi \cdot (d^2 - d_1^2)}, \quad (7)$$

so result stress is equivalent to:

$$\sigma = \sqrt{\sigma_s^2 + 3 \cdot \tau^2}. \quad (8)$$

Values of the result loads at extreme rotation positions ($\varphi_1=0^\circ$ and $\varphi_1=90^\circ$) and values of stresses obtained by analytic method using relations given in this paper are presented at Tab. 1. The values of the stresses that are obtained with neglecting the stresses concentrations are not relevant, so numeric calculations of stresses must be done.

Table 1: Load at cross shaft as function of variation of operation angle α_{12} in extreme positions

α_{12} [°]	$T_{\alpha_{12}}$ [Nmm]		F [N]		σ_z [MPa]		τ [MPa]		σ [MPa]	
	$\varphi_1 = 0^\circ$	$\varphi_1 = 90^\circ$	$\varphi_1 = 0^\circ$	$\varphi_1 = 90^\circ$	$\varphi_1 = 0^\circ$	$\varphi_1 = 90^\circ$	$\varphi_1 = 0^\circ$	$\varphi_1 = 90^\circ$	$\varphi_1 = 0^\circ$	$\varphi_1 = 90^\circ$
0	159166.67	159166.67	3031.75	3031.75	68.26	68.26	12.53	12.53	71.63	71.63
10	156748.57	161622.07	2985.69	3078.52	67.22	69.31	12.34	12.73	70.54	72.74
20	149567.74	169381.63	2848.91	3226.32	64.14	72.64	11.78	13.34	67.31	76.23
30	137842.38	183789.84	2625.57	3500.76	59.12	78.82	10.85	14.47	62.03	82.71
40	121928.74	207777.33	2322.45	3957.66	52.29	89.11	9.60	16.36	54.87	93.51
50	102310.36	247619.38	1948.77	4716.56	43.88	106.20	8.06	19.50	46.04	111.44
55	91294.25	277498.62	1738.94	5285.69	39.15	119.01	7.19	21.85	41.08	124.88

2.2 Calculation of stresses by numeric method

The design and process of project development of power transmitter with Cardan joint must be done with great care due to the set of constructional requirements that must be fulfilled by design solution. The results obtained by analytic calculations cannot take as relevant in all cases because those calculations are done on simplified model. The method of numeric calculation by finite element analysis is the one of the methods that provides calculations on the mathematical models with real geometry.

The analysis by FEM method is much more precise in relation to analytic method. The finite element method provides possibility of fast repeated calculations after modifications of some design details of considered element. In this paper the simulation of load at cross shaft done using the software package *Autodesk Inventor Professional 2011* is presented. The analysis by finite element method require following procedure [7]: creation of geometric model, definition of material, discretization by finite elements, definition of support location and load limitations, the specification of location and characteristic of load, numeric calculation and interpretation of results.

The basic considered model for analysis by FEM method in this paper is created upon the cross shaft. Geometric model made by Computer Added Design software packet is formed from simple geometrical shapes called geometric forms. The geometric model defines the real geometry of the considered element. The material of the all considered models in this paper is steel with following characteristic: elastic modulus $E=2.07 \cdot 10^5$ MPa, Poisson’s ratio $\nu=0.287$.

The three dimensional tetrahedral discretization with density variation is done at first stage of numerical model generation. The zone of shape transition as zone of interest is discretized by the finite elements with smallest dimensions (Fig. 6) [9].

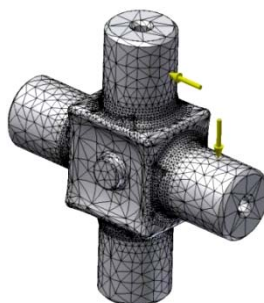


Figure 6: Discretization of numerical model

The border conditions are defined in according to theoretical considerations of stress state at cross shaft. The cross shaft is element with symmetry and four branches. The axes of the branches are in the same plain, forming the angle of 90° by them. The every branch is loaded by the same force transmitted from the yoke by the bearings. In the reference [4] numeric analysis is done for quarter of the cross shaft, only one branch loaded by one of the forces, but the numeric analysis in this paper is done for the whole cross shaft. The central zone is fixed and the each branch is loaded by the force in the interval from 30.3 kN to 52.8 kN and variations of stresses on the basis of the branches of the cross shaft are analyzed, as consequence of variation of operation angle α_{12} and rotation angles φ_1 and φ_2 .

In order to numeric calculation has been done, it is necessary to repeat the procedure of structural analysis for every value of operation angle α_{12} . The every analysis is done for different rotation position of shafts defined by rotation angle φ_1 in interval between $\varphi_1=0^\circ$ and $\varphi_1=180^\circ$ due to symmetry of results from the position corresponding to half of the one rotation. Visualizations of results of calculations of stresses for different operating angles α_{12} and different rotation angle φ_1 are presented at Fig. 7, Fig. 8, Fig. 9, Fig. 10, Fig. 11 and Fig. 12.

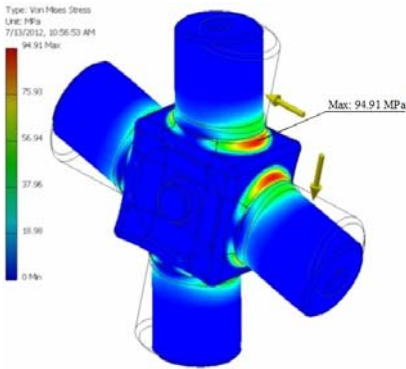


Figure 7: Numeric analysis of stresses at cross shaft for angles $\alpha_{12}=10^\circ$ and $\varphi_1=0^\circ$

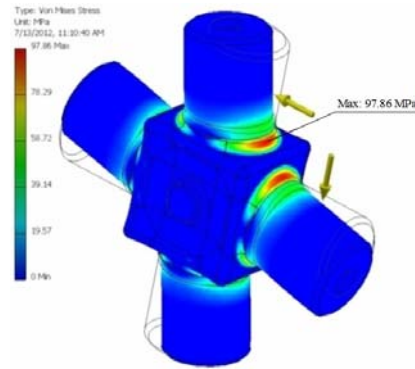


Figure 8: Numeric analysis of stresses at cross shaft for angles $\alpha_{12}=10^\circ$ and $\varphi_1=90^\circ$

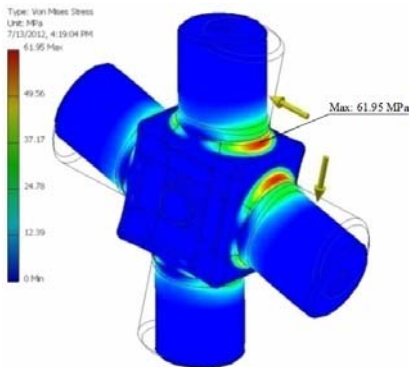


Figure 9: Numeric analysis of stresses at cross shaft for angles $\alpha_{12}=50^\circ$ and $\varphi_1=0^\circ$

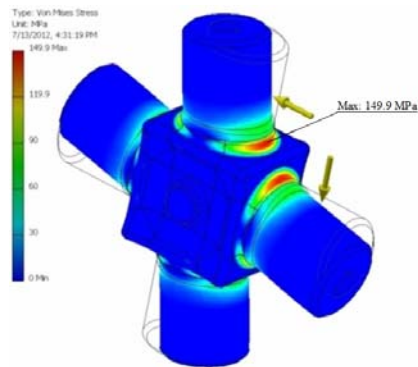


Figure 10: Numeric analysis of stresses at cross shaft for angles $\alpha_{12}=50^\circ$ and $\varphi_1=90^\circ$

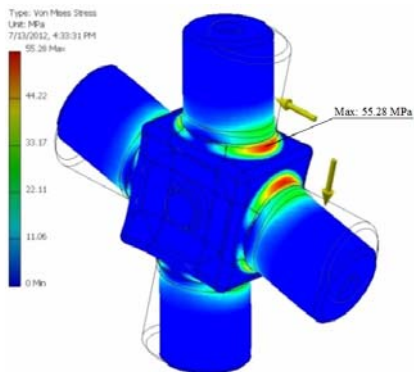


Figure 11: Numeric analysis of stresses at cross shaft for angles $\alpha_{12}=55^\circ$ and $\varphi_1=0^\circ$

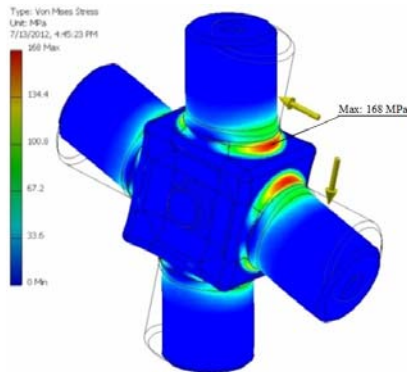


Figure 12: Numeric analysis of stresses at cross shaft for angles $\alpha_{12}=55^\circ$ and $\varphi_1=90^\circ$

3. GRAPHICAL PRESENTATION AND ANALYSIS OF CALCULATION RESULTS

The referent values of result stresses determined by analytic and numeric methods are presented at Fig. 13.

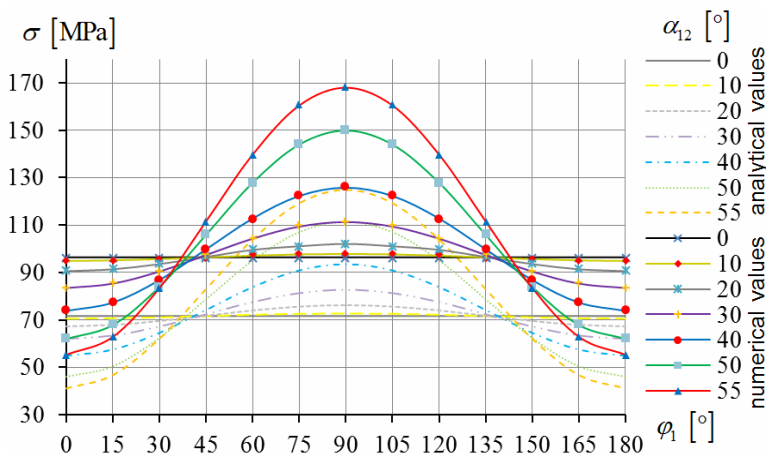


Figure 13: Results of analytical and numerical calculations of maximal stresses as functions of rotation positions

Referent analysis of result stresses obtained by analytic and numeric methods are based on values of relative variations expressed in % that are calculated in following form:

$$\Delta\sigma = \frac{|\sigma - \sigma^*|}{\sigma^*} 100 [\%], \tag{9}$$

where is: $\Delta\sigma$ – relative variation of considered value, σ – value obtained by numeric method, σ^* – value obtained by analytic method. The compare presentation of relative variations of result stresses obtained by numeric method in relation to values obtained by analytic method is given at Fig. 14. To the aim of clear presentation of those variations every value from the considered interval of corresponding angle α_{12} is divide by corresponding value that is obtained for rotation angle $\varphi_1=0^\circ$.

This presentation implicates that calculation of stresses by numeric method for different rotation angles have small differences from the values calculated by analytic method and that those differences are in allowable limits.

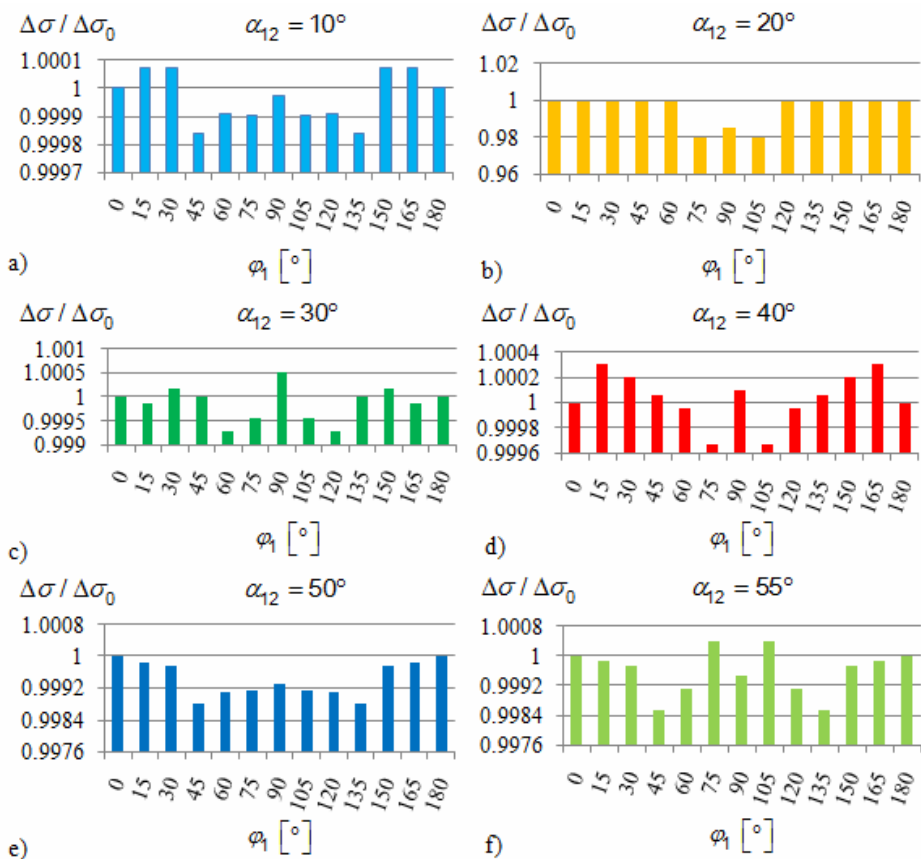


Figure 14: Variation of result stress for different values of angle α_{12}

The variation of result stress in function of variation of angles α_{12} and φ_1 are illustrated at Fig. 15.

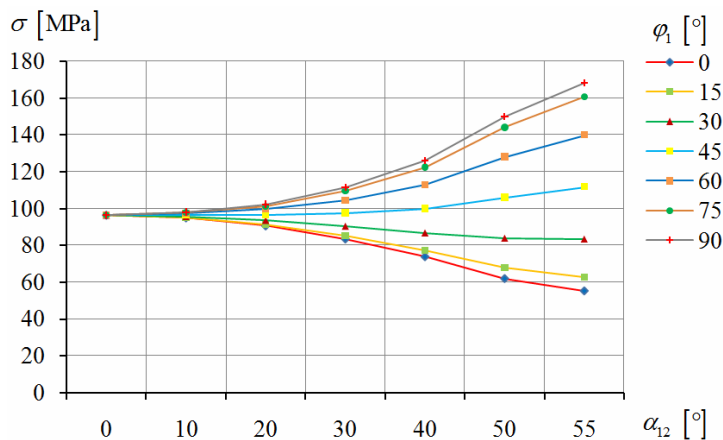


Figure 15: Variation of result stress in function of different values of angles α_{12} and φ_1

With increase of angle α_{12} the result stress also increase but only for higher values of rotation angle φ_1 ($\approx 45^\circ$ and higher). For the angles φ_1 smaller than ($\approx 45^\circ$) the decrease of result stresses are induced. The presentation at Fig. 15 also implicate the identification of angles that cause severe variation of stresses and it is, by that, recommended to avoid exploitation of Cardan shafts with those values of operating angles.

CONCLUSIONS

On the basis of the conducted analysis of the results the following conclusion can be done:

- Diagrams of stresses obtained by numeric and analytic method are of the same variation forms that implicate that established model for numeric analysis are done on the base of correct constructional solution and obtained results can be taken as relevant for further analysis in this area in order to minimize the stress level, so as for dynamic and fatigue analysis.
- Value of stresses obtained by numeric calculation are higher that results obtained by analytic method due to neglecting stress concentration for analytic method. The real shape transition zone from the central part to the branches at cross shaft is complex geometric form that provoked stress concentration and for precise determination of stresses the numeric analysis that considered real geometry must be done.

Maximal values of stresses are obtained for the operation angles α between input and output shaft of $\alpha_{12}=55^\circ$ and for rotation angle of $\varphi_1=90^\circ$.

On the basis of the conclusions it can be stated that both analytic and numeric method provide relevant results for analysis of stress variation due to changing of the input parameters, but special care must be put on problems of motion and relative positions of certain elements in exploitation. The influence of variation in positions of Cardan power

transmitter elements is significant to variation of stresses at critical cross section at the basis of the branches at cross shaft.

ACKNOWLEDGMENTS

Financial support for the work described in this paper was provided by Serbian Ministry of Education and Science, project (TR35033).

REFERENCES

- [1] Bayrakceken, H.; Tasgetiren, S. & Yavuz, I.: “Two cases of failure in the power transmission system on vehicles: A universal joint yoke and a drive shaft”, *Engineering Failure Analysis* 14, 2007, pp. 716–724, ISSN: 1350-6307
- [2] Humell, R. S. & Chassapis, C.: “Configuration design and optimization of universal joints”, *Mechanism and Machine Theory*, Vol. 33, No. 5, 1998, pp. 479-490, ISSN: 0094-114X
- [3] Humell, R. S. & Chassapis, C.: “Configuration design and optimization of universal joints with manufacturing tolerances”, *Mechanism and Machine Theory*, Vol. 35, 2000, pp. 463-476, ISSN: 0094-114X
- [4] Ivanović, L.; Josifović, D.; Živković, K. & Stojanović, B.: “Cross Shaft Design From the Aspect of Capacity”, *Scientific Technical Review*, Vol.61, No.1, 2011, pp. 48-53, ISSN: 1820-0206.
- [5] Ivanović, L., Josifović, D., Rakić, B. Stojanović, B., Ilić, A.: “Shape Variations Influence on Load Capacity of Cardan Joint Cross Shaft”, *The 7th International Symposium KOD 2012, Machine and Industrial Design in Mechanical Engineering*, 24 - 26 May 2012, Balatonfüred, Hungary, Proceedings, pp. 205-210
- [6] Jovičić, S., Marjanović, N.: “The basics of machine design”, Faculty of Engineering, University of Kragujevac, 2011, ISBN: 978-86-86663-81-8, Kragujevac (in Serbian)
- [7] Kojić, M.; Slavković R.; Živković, M. & Grujović, N.: “Finite Element Method I (linear analysis)”, Faculty of Mechanical Engineering, 2010, ISBN: 86-80581-27-5, Kragujevac (in Serbian)
- [8] Rathi, V. & Mandavgade, N. K.: “FEM analysis of universal joint of Tata 407”, *Second International Conference on Emerging Trends in Engineering and Technology, ICETET-09*, 2009, pp. 98-102.
- [9] Rakić, B.: “Modelling and simulation of power transmitter with Cardan joints”, Degree project, Faculty of Mechanical Engineering, 2011, Kragujevac (in Serbian)
- [10] Seher-Thoss, H. C., Schmelz, F., Aucktor, E.: “Universal joints and driveshafts: analysis, design, applications”, 2006, Birkhäuser, ISBN: 9783540301691
- [11] Tanasijević, S.: “Power transmitters”, *Yugoslav Tribology Society*, 1994, ISBN: 86-23-43041-7, Kragujevac (in Serbian)
- [12] <http://www.sdp-si.com/D757/couplings3.htm>, downloaded 14.07.2012

MVM Editorial Board
University of Kragujevac
Faculty of Engineering
Sestre Janjić 6, 34000 Kragujevac, Serbia
Tel.: +381/34/335990; Fax: + 381/34/333192
www.mvm.fink.rs